CHALMERS
UNIVERSITY OF TECHNOLOGY

Waste Heat Recovery Simulation Model based on the Rankine Cycle for Passenger Cars applications

Development of a Computational Model in SIMULINK

Master's thesis for the Degree of Master of Science

Gustav Haby
Carlos Ramirez

Department of Applied Mechanics
CHALMERS UNIVERSITY OF TECHNOLOGY
Gothenburg, Sweden 2017

Master's thesis 2017:68

Waste Heat Recovery Simulation Model based on the Rankine Cycle for Passenger Cars applications

Development of a Computational Model in SIMULINK

Gustav Haby
Carlos Ramirez

CHALMERS
UNIVERSITY OF TECHNOLOGY

Department of Applied Mechanics
Division of Combustion
Chalmers University of Technology
Gothenburg, Sweden 2017

Waste Heat Recovery Simulation Model based on the Rankine Cycle for Passenger Cars applications
Development of Computational Model in SIMULINK
Gustav Haby, Carlos Ramirez

Supervisor: Fredrik Ekström, Volvo Car Corporation
Examiner: Sven Andersson, Department of Applied Mechanics

Master's Thesis 2017:68
ISSN 1652-8557
Department of Applied Mechanics
Division of Combustion
Chalmers University of Technology
SE-412 96 Gothenburg
Telephone +46 31 772 1000

Typeset in LaTeX
Printed by Chalmers Reproservice
Gothenburg, Sweden 2017

Waste Heat Recovery simulation Model based on the Rankine Cycle for Passenger Cars applications based on the Rankine Cycle
Development of a Computational Model in Simulink
Gustav Haby & Carlos Ramirez
Department of Applied Mechanics
Chalmers University of Technology

Abstract

The demand for more energy efficient passenger cars is steadily increasing due to increasing fuel prices, future emission regulations and awareness of the effects that the emissions of carbon dioxide has on the climate. As a large portion of the fuel energy in internal combustion engines is lost as heat, ways of utilizing more of this waste heat has gained interest in recent years. The most promising method to recover waste heat for automotive applications is with assistance of the Rankine cycle.

The exhaust temperature and flow of exhaust gases are highly variable and hence the modeling of a Rankine based waste heat recovery system is of transient nature. To accurately predict the heat energy that is possible to utilize careful modeling of the heat exchanging devices is of utmost importance. Especially the prediction of evaporation in the boiler is important since steam engines requires saturated steam conditions to work efficiently. Direct transmission of mechanical energy to the powertrain demands that the expander speed and motor engine speed is matched, which creates a dynamic system where the pump pressure has to be controlled.

This thesis has investigated the possibilities to mathematically model a waste heat recovery system for passenger cars with the help of the model based software SIMULINK and the fluid library CoolProp. The results shows that it is beneficial to recover waste heat through a Rankine system. The waste heat efficiency achieved were found to be 2.85% for city driving, 5.00% for country roads and 5.02% for free ways. These results were achieved for a gear ratio of 1.5:1, which was found to be the best ratio.

Keywords: Waste heat recovery, heat exchanger, evaporator, SIMULINK, Rankine cycle, expander, finite volume method(FVM), two-phase modeling, CoolProp.

Acknowledgements

First and foremost we wish to acknowledge our supervisor Fredrik Ekström at Volvo Car Corporation and thank him for great support and feedback during the journey of finishing this master's thesis. We would also like to express our gratitude to group manager Stefan Dunert at Volvo Cars. Thanks to our examiner and supervisor at Chalmers, Sven Andersson. We are also very grateful for the technical input regarding heat exchanger design and the fluid library CoolProp that we have received from Jelmer Rijpkema at Chalmers. Thanks to Robert Ulmehag for technical support with SIMULINK.

Gustav Haby, Camilo Ramirez

Gothenburg, June 2017

Contents

List of Figures

List of Tables

1

Introduction

The automotive industry today is facing big challenges due to environmental concerns related to the emissions of carbon dioxide. The emissions of carbon dioxide is contributing to an increased intensity in the green house effect which is the cause of global warming. New emission regulations such as EU-6D, increasing fuel prices and a customer demand for more environmental friendly cars is putting pressure on the industry to make a transition from internal combustion engines towards less carbon intensive alternatives such as hybrid-, electric- or fuel cell drivelines.

Since only 25% of the fuel energy in an internal combustion engine becomes brake power and 40% is lost as heat, measures of increasing the efficiency has also drawn attention in the industry[1]. The most promising measure of waste heat recovery is through a Rankine cycle based system, although other methods exist for example thermoelectric systems, using the Peltier-Seebeck effect. Waste heat recovery system for automotive application has been widely investigated by different authors. In a literature review of automotive heat recovery system by Spouse et al. heat recovery efficiencies for organic Rankine cycles demonstrates results in the range 15 to 20%. However these numbers seem to be in excess of what is realistically possible since heat loss to the ambient often is not accounted for. More realistic numbers of waste heat efficiency range from 7-10%, which approximately can be translated into similar numbers of fuel savings, although there are some small drawbacks in horse power losses caused by an increased back pressure due to the waste heat appliances.[2]

In an ideal Rankine cycle a working medium is compressed isentropically to raise the pressure of the fluid, after which the fluid is heated and evaporated by a heat source, followed by an isentropic expansion before it is finally condensed back to its initial state[3]. The purpose of using the Rankine cycle is to lower the fuel consumption of the vehicle. This thermodynamic cycle can assist the engine by putting the output from the expander back into the driveline. The energy for this operations is taken from the waste heat in the exhaust gases and the produced work can either be used directly in the driveline or potentially be converted into electrical energy for hybrid solutions.

The choice of working fluid in a waste heat recovery system is crucial as different fluids have widely different thermodynamical properties. A proper investigation of organic fluids suitable for waste heat recovery applications for cars have been

performed by Wang et al. The thermal efficiencices and exergy destruction rates were investigated. [4]

1.1 Purpose

The purpose of this master's thesis is to develop a Rankine based waste heat recovery computation model in SIMULINK and investigate the thermodynamic behavior of the cycle and its efficiency.

1.2 Objective

The main objective of the project is to create a simulation model solid enough to evaluate different load cases based on different driving fields. The model will be built as a simple Rankine cycle, with ethanol as the working medium, however the aim is a generic model that could be easily extended to different fluids and compression ratios. The model will contain of four components constructed separately by mathematical models implemented in SIMULINK.

The fair amount of stainless steel in the heat exchanger walls stores a lot of heat energy that has to be taken into consideration and makes the model transient. This will give a delay in the system that also has to be implemented in the simulation model. The system pressure will be a function of both the heat transferred to the working fluid and the speed of the expander. Therefore the speed of the pump has to be controlled to match the system pressure that arises.

1.3 Delimitation

Only Rankine based waste heat recovery system will be considered. Validation of the model against experiments will not be performed.

2

Thermodynamics related to the Rankine Cycle

Thermodynamics is defined as the science of energy and governed by the four laws of thermodynamics. It is an essential subject to grasp in order understand how heat engines work and operate. In the following chapter the theoretical framework of subjects that are essential to this project will be explained and visualized. As a background basic thermodynamics, the laws of thermodynamics and the working of heat engines including the theoretical Carnot cycle and the widely used Rankine cycle will be covered. Further, the modes of heat transfer, which are essential for setting up the correct heat balance, when analyzing heat exchangers is dealt with. The choice of working fluid in a Rankine cycle is important for the efficiency of Rankine system and will be investigated. Finally the different components making up the Rankine cycle will be explained in depth.

2.1 Laws of thermodynamics and control volume formulation

There are four essential laws describing the behaviour of a thermodynamic process. The conservation of energy principle states that energy can only change form from one to another, but that the total energy in a given system will remain the same. Put in other words this means that energy cannot be created nor destroyed. The first law of thermodynamic is based on the law of conservation of energy. This law provides an essential function to perform calculations of heat rate transfer, by identifying a so called control volume and applying the conservation of energy principle to it. A control volume is bounded by a surface where mass or energy may pass. An example of such a control volume is shown in figure 2.1. It has one side where the energy enters and another side where the energy leaves the control volume. The control volume formulation of the first law of thermodynamics states that *"The amount of thermal and mechanical energy that enters a control volume, plus the amount of thermal energy that is generated within the control volume, minus the amount of thermal and mechanical energy that leaves the control volume must equal the increase in the amount of energy stored in the control volume"*[3]. This formulation must be

specified over a certain time interval. A typical way for the heat energy to enter and leave the control volume is by conduction, convection or radiation. These three modes of heat transfer will be explained in depth later.

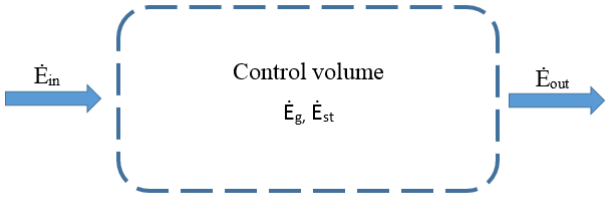

Figure 2.1: *A control volume where energy or mass may pass the boundaries*

The first law of thermodynamics tell us about the energy quantity that are transported, taking no consideration to its quality or direction of travel. To make sure that a heat transfer process is going to take place, a second law has to be considered, namely the second law of thermodynamics. It states that heat transfer process spontaneously travels in a certain direction, which is from a hotter medium to a colder medium. Another formulation of the second law of thermodynamics states that the entropy of a system always increases which is equivalent to that the energy quality, or exergy, is decreasing. This is a major problem for engineers and by the second law of thermodynamics it is possible to determine the quality and the degradation of the energy while going through the system. [3]

To complete the whole thermodynamic process the zeroth and third laws are defined. The zeroth law pronounces that *if two systems have the same temperature as a third one, the two system have equal temperatures* [5, pp.55]. In other words, two mediums with different temperatures will always aim to get into thermal balance. Lastly the third law of thermodynamics states that the entropy at the absolute zero for a crystalline structure is zero and nonzero for substances not having a crystalline structure[6].

2.2 Heat engines

A heat engine converts thermal energy to mechanical work by taking heat from a source, with high temperature, to a sink with lower temperature (Figure 2.2). Work is produced with the help a work producing machine as heat is transferred through a working medium from the source to the sink. From now on the type of heat engines considered are engines with a fluids as working mediums that produces work as they flow through a system. The fluid is heated up and returned to its initial state as they flow through the system in a cyclic manner[3]. The heat engine operating in this project belongs to the class of steam power engines(Figure 2.3a). Unfortunately the heat transfer process has a lot of heat losses during the cycle and a lot of effort

is put in, in order to minimize these losses. The laws of thermodynamics covered previously dictates the heat losses produced during the cycle.

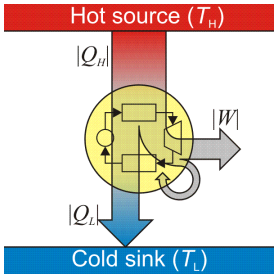

Figure 2.2: *The picture visualizes the thermodynamic behaviour of a heat engine as work is produced while heat is transported from a heat source to a sink. Distributed under a CC BY-SA 3.0 License*

2.2.1 The Carnot cycle

The Carnot cycle is the most efficient cycle operating between two specified temperatures. It is based on the work of the french physicist Nicolas Leonard Sadi Carnot(1796-1832), who stated that *"two reversible heat engines operating between equal heat sources and heat sinks have identical thermal efficiencies"*. The Carnot cycle is considered an ideal cycle, which means that no heat or friction losses is present. Processes having these properties are termed isentropic.

The efficiency of a Carnot cycle depends on how the individual processes(components), that constitutes the cycle operates. To obtain the maximum possible net work and efficiency from the cycle requires that the amount of work put into the cycle is at a minimum and that the delivery of work is the highest possible. This requires that the processes of all the individual components are reversible[3]. If a cyclic process is reversible it means that an ideal process, would bring the system and its enclosing to the exact same condition as its initial state without losses. The net heat and the net work exchange between the cycle and its surrounding is zero[5]. A system is called irreversible if the system and all parts of its surrounding cannot be restored to the initial state. Typically irreversibilities in a cyclic process can be, unrestrained expansion of a medium to a lower pressure, friction, heat transfer through a finite temperature difference or chemical reactions. The Carnot cycle is only of theoretical nature, as reversible processes do not exist in real life, but serves well as a tool when comparing different working cycles.[6, pp.195-200]. The theoretical efficiency of the Carnot cycle is

$$\eta_c = \frac{W}{Q_h} = 1 - \frac{T_c}{T_h} \tag{2.1}$$

where W is the net work output, Q_h is the heat input, T_c is the sink temperature and T_h is the source temperature.

Figure 2.3b shows the Carnot vapor cycle and the different states of temperate and entropy and figure 2.3a visualizes a simple steam power expander cycle constructed by the four most essential components.

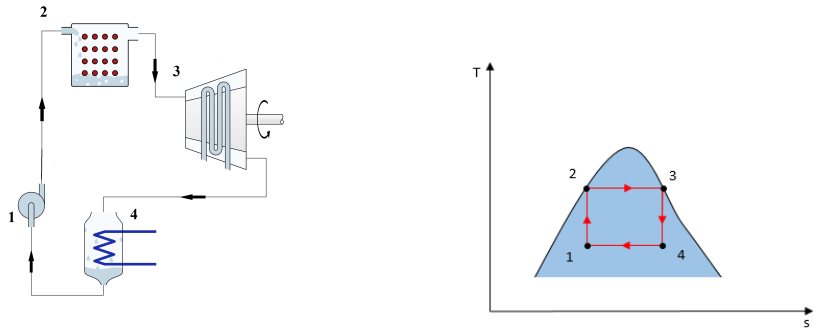

(a) *Steam power expander cycle. Distributed under a CC BY-SA 4.0 License* **(b)** *Carnot cycle*

Figure 2.3: *Temperature and entropy diagram of the ideal Carnot Vapor Cycle*

Looking at figure 2.3b, where the different stages of the Carnot cycle is visualized the working of the cycle is as follows:

- **1-2 Isentropic compression:** The fluid is compressed isentropically, which causes the temperature to increase from T_1 to T_2. The compression device is assumed frictionless and thermally insulated.
- **2-3 Isothermal heat addition:** The fluid is isothermally expanded causing a phase change and an increase in entropy. Heat is added at a constant temperature equal to the temperature of the source.
- **3-4 Isentropic expansion:** The fluid is isentropically expanded giving a useful work output equal to the decrease in internal energy of the fluid. The temperature decreases to the temperaure of the sink.
- **4-1 Isothermal heat rejection:** The fluid is isothermally expanded causing a phase change and a decrease in entropy. Heat is rejected at a constant temperature equal to the temperature of the sink.

There are some disadvantage and unwanted effects that occur through the different stages, for instance that the steam quality decreases during the isentropic expansion process. This behaviour will increase the moisture content which in turn will generate small liquid drops causing erosion on the turbine blades and decreasing the cycle efficiency[3, pp.564]. Another problem is the isentropic compression from stage one to stage two since it is complicated to obtain the desired quality of saturated liquid after the compressor. There is also a temperature limit when working with a two-phase cycle, where the limit depends on the working fluid. By instead using the Rankine cycle (Figure2.4) as an alternative choice, can all of these unwanted effects

be reduced. (Fig.2.4).[7, pp.332] [3, pp.556-557]

2.2.2 The Rankine cycle

The Rankine cycle, after the Scottish engineer William Rankine, is the theoretical cycle describing the function of steam cycles. The thermodynamic principles that have been explained are continuously acting through the whole cycle process. These laws applies to different parts of the cycle. For instance the second law of thermodynamics is an essential rule for the functionality of the heat exchanger and the condenser. At the same time the conservation of mass and energy is fundamental for calculations and analysis of the cycle. [6, pp.349]

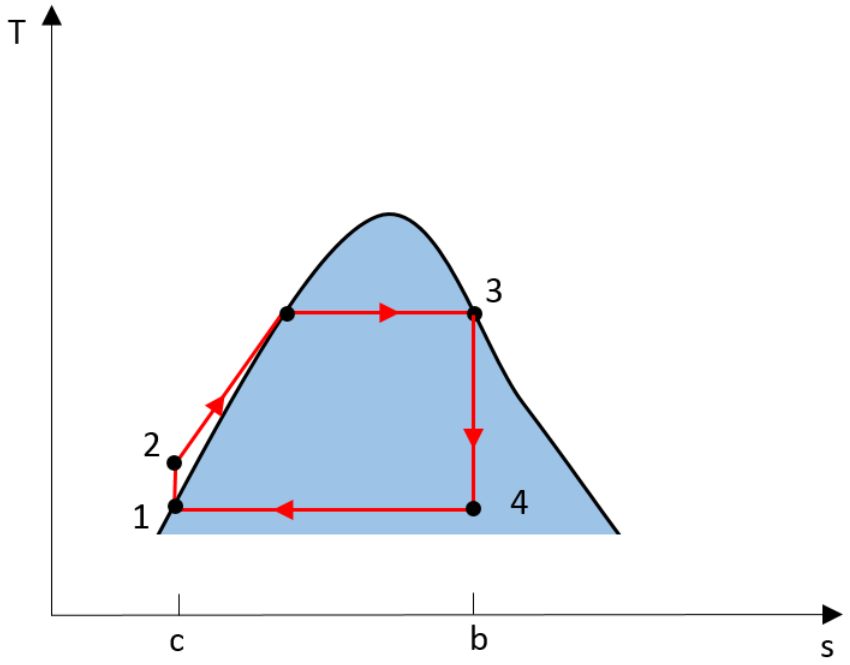

Figure 2.4: *Temperature and entropy diagram of the ideal Rankine vapor cycle*

The ideal Rankine cycle has the same thermodynamic assumptions as the ideal Carnot cycle, which means a cycle process without irreversibilities. There are no frictional pressure drop in the boiler and the condenser and the fluid flows isentropically through the pump and expander[6, pp.351]. The process steps in the Rankine cycle are similar to those in the Carnot cycle(Figure 2.4). These steps are going to be explained below

- **1-2 Isentropic compression:** The fluid that is in saturated liquid phase is pumped from low to high pressure isentropically. It is favourable that the fluid is in liquid form as the work input needed to raise the pressure a certain amount is much smaller compared to the work input that would have been

needed if the fluid were in the two-phase area.

- **2-3 Isobaric heat addition:** The fluid is heated isobarically and evaporated causing a phase change and an increase in entropy.
- **3-4 Isentropic expansion:** The fluid is isentropically expanded giving a useful work output equal to the decrease in internal energy of the fluid.
- **4-1 Isothermal heat rejection:** The fluid is condensed isobarically and isothermally back to its initial state. Heat is rejected at a constant temperature.

The thermal efficiency of the Rankine cycle is

$$\eta = \frac{(h_3 - h_4) - (h_2 - h_1)}{h_3 - h_2} \tag{2.2}$$

where h is the enthalpy at the different stages in the cycle.

2.2.3 Improvements of the Rankine cycle

There are some typical ways to modify the Rankine cycle in order to increase its efficiency and functionality[6, pp.362][3, pp.564][5, pp.164]. The whole purpose of these modifications are to *"Increase the average temperature at which heat is transferred to the working fluid in the boiler, or decrease the average temperature at which heat is rejected from the working fluid in the condenser"* [3, pp.564]

By lowering the condenser pressure the temperature will decrease as shown in figure 2.5a and the net output will increase. A drawback with this modification is that the driving temperature difference in the condenser decreases yielding a less effective heat transfer[3, pp.564].

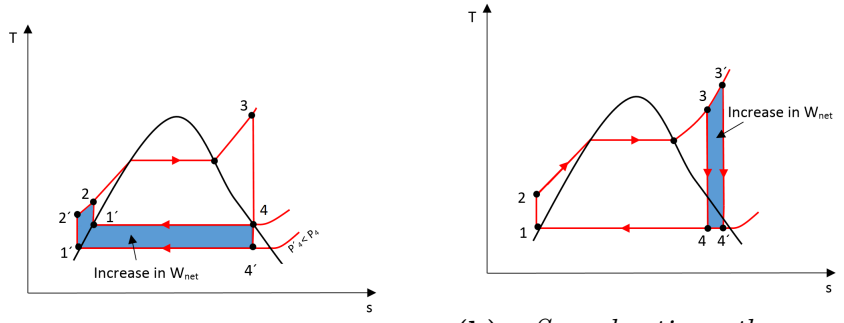

(a) *Lowering the condenser pressure yields a higher net output.*

(b) *Superheating the working fluid can decrease the moisture content in the expander*

Figure 2.5: *Modification of the Rankine cycle visualized in a temperature-entropy diagram*

The amount of moisture after the expander can be reduced by superheating the fluid [5, pp.164][6, pp.362]. Superheating is based on adding more heat to the steam which leads to a superheated vapor condition [6, pp.362] and a higher average temperature without increasing the pressure in the boiler [3, pp.564]. The effect obtained by increasing temperature is, higher thermal efficiency which means higher work output (Figure 2.5b). Working with high temperature levels requires materials that can handle such high levels, therefore limitations of superheating exist, dependent on the capability of the material.[3, pp.564]

2.2.4 Modes of heat transfer

As mentioned before, heat travels from one medium to another by convection, conduction and radiation. Normally these three phenomena act at the same time. It can for instance start with cold air blowing on a hot surface where the heat transfers occurs by convection. The energy obtained through convection will travel through the medium by conduction until both mediums get into thermal balance. Radiation depends on the type of surfaces acting with each other, and will perform in different intensity depending on the surfaces emissive power. The energy of the radiation is transported by electromagnetic waves, which means that radiation transfer transfers best in vacuum, while transferring energy by convection and conduction needs a material to exchange the energy between the different mediums.[8, pp.2-11]

2.2.5 Convection

Convection is the energy transfer between a solid surface and a liquid or a gas in motion, where a large numbers of molecules are moving together in a bulk. The fluid motion has a big influence on the heat transfer. The faster the fluid motion

travels the greater the convection transfer. This fact is used in forced convection, where an external source such as a fan or pump is used to increase the speed of the bulk flow. Forced convection is vital for the design of heat exchangers. As opposed to forced convection where an external source is used to force the convection, density differences leading to temperature gradients drives the heat transfer in natural convection. [5][3, pp.106-111] [8][9]

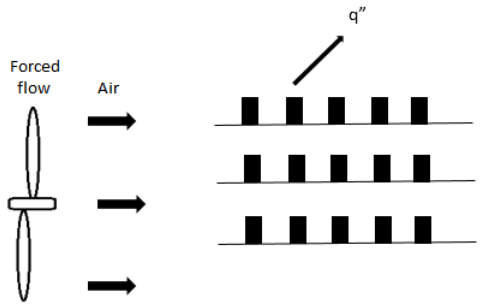

Figure 2.6: *Forced Convection*

2.2.6 Conduction

Conduction occurs in an atomic level and may be viewed as energy that transfers between particles. The energy goes from more energetic to the less energetic particles[3, pp.106], which means that heat goes from high to low temperature like the second law of thermodynamics pronounces. In gas and liquid the conduction takes place due to collisions between the molecules during random motion while in solids, the conduction is due to vibrations of molecules and energy transported by electrons. [3, pp.106] [8, pp.3]

2.3 Components of the Rankine Cycle

In the following section the different components of the Rankine system will be explained. Especially the effects of choice of expander and heat exchanger will be deeply investigated as they are crucial components for a realistic model of a waste heat recovery system. The choice of working fluid will also be covered as it has proved to be an important parameter for the overall efficiency of waste heat recovery systems.

2.3.1 Compression device

Compression of a fluid is done with the help of a work absorbing device that raises the pressure of the fluid. If the fluid is a flowing liquid the device is usually denoted

a pump. In this chapter pumps will be considered as liquid is the working state when compressing the fluid in a Rankine Cycle. There are a lot of classification of pumps but one distinctive classification is to differentiate between reciprocating pumps and rotary pumps. Pumps consume energy to operate and the aim is to transfer a major part of this energy to the fluid by increasing its pressure so that a flow can be achieved. The enthalpy increase in the pump with the notations used in figure 2.4 is

$$\frac{\dot{W}_p}{\dot{m}} = h_2 - h_1 \tag{2.3}$$

2.3.2 Heat exchanger

A heat exchanger is a device that transfer heat from a warmer fluid to a colder fluid. The heat transfer could occur either directly through mixing, or indirectly if the fluids are separated by a wall or membrane. The heat transfer in a heat exchanger is governed by the law of conservation of energy, momentum and mass. The basics are described in the following section based on the chapter about heat exchangers by Allan D. Kraus in the Heat Transfer handbook[9]. Assuming two separated fluid streams of different temperatures denoted T_{hot} and T_{cold}, the heat heat transfer per square meter separating material between the two fluid can be described as

$$q^{''} = C_h(T_{h,i} - T_{h,o}) = C_c(T_{c,o} - T_{c,i}) \quad [W/m^2] \tag{2.4}$$

where $C_h = \dot{m}_h C_{p,h}$ and $C_c = \dot{m}_c C_{p,c}$ are the heat capacity rates. Equation 2.4 represents an ideal case where there are no heat losses and it does not take the size of the device into account. If the size of the heat exchanger is included in equation 2.4 it can be rewritten as

$$\dot{q} = UA\Delta\theta = U_h A_h \Delta\theta = U_c A_c \Delta\theta \quad [W] \tag{2.5}$$

which is the heat transfer between the two fluids, where U_* are the overall heat transfer coefficients and $\Delta\theta$ is the driving temperature difference normally the logarithmic- or arithmetic temperature difference. The overall heat transfer coefficient is related to to the heat transfer coefficients as

$$U = \frac{1}{\frac{A}{\alpha_h A_h \eta_h} + \frac{A}{\alpha_{hf}\eta_h} + AR_m + \frac{A}{\alpha_{cf} A_c \eta_c} + \frac{A}{\alpha_{cf}\eta_c}} \tag{2.6}$$

where every quotient is a thermal resistance, that is a difficulty that has to be overcome, when the heat is transferred from the source to the sink. α_h and α_c are

the convective heat transfer coefficient for the hot and cold side respectively, whereas α_{hf} and α_{cf} are the fouling heat transfer coefficient. Fouling is the accumulation of undesirable particles that increases the thermal resistance. The term R_m represents the resistance of the material separating the streams and for a tubular geometry it is written as

$$R_m = \frac{ln\left(\frac{d_o}{d_i}\right)}{2\pi k_m L} \tag{2.7}$$

where k_m is the thermal conductivity of the tube material. To obtain a large heat transfer surface area per unit volume fins can be introduced. The fin efficiency is included in equation 2.6 denoted η and is set to one if there are no fins.

Heat exchangers can be classified according to the flow configuration, as either counter- or parallel flow heat exchangers. The configuration of a counter current heat exchanger is shown in figure 2.7a and figure 2.7b whereas the configuration of a cocurrent heat exchanger can be seen figure 2.8a and 2.8b. The counter current construction generates a higher heat transfers efficiency compared to the parallel flow heat exchanger where the fluids travels in the same direction. The Temperature difference is larger for the parallel flow heat exchanger at the beginning compared to the counterflow, hence there is an initial large driving force for heat transfer, that however will decrease swiftly along the flow direction. The counter flow configuration has a more stable temperature difference giving a high heat transfer throughout the flow direction.[8, pp.642-651]

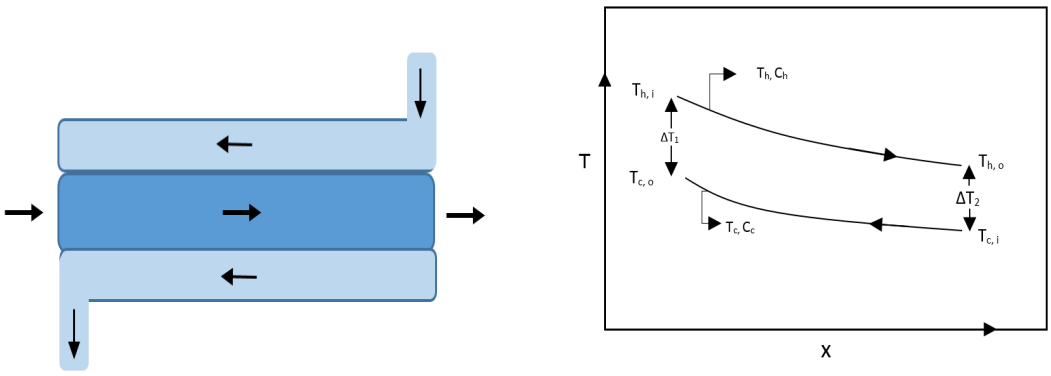

(a) *Heat exchanger with counter flow configuration.*

(b) *Temperature distribution along the flow direction in a counter current heat exchanger.*

Figure 2.7: *Counter current heat exchangers are more efficient than their counter part.*

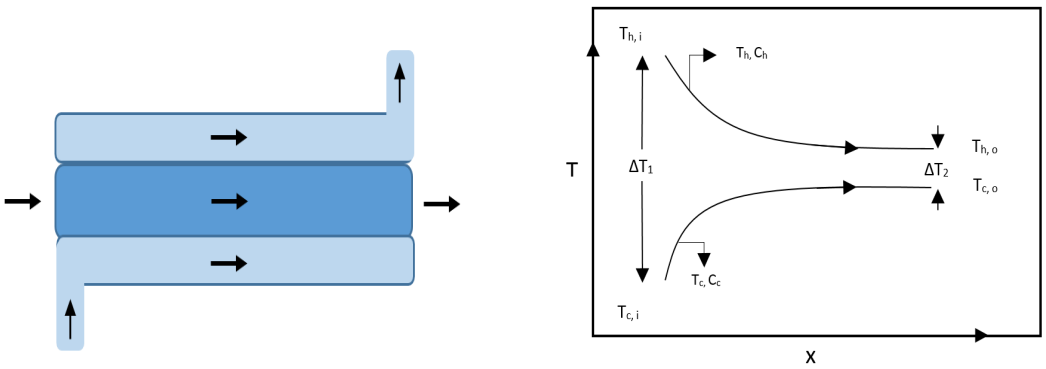

(a) *Heat exchanger with parallel flow configuration.*

(b) *The driving temperature is high in the beginning of the heat exchanger but decreases throughout.*

Figure 2.8: *Schematics and temperature distribution of a counter flow heat exchanger.*

The helical-coil heat exchanger is operating in a counter flow configuration. This choice of heat exchanger is the ideal design for situations where the assembly space is limited, as well as the pressure drop of the working fluid. It can also be used where laminar flow is common or low flow rates are expected and where the resulting low heat transfer coefficients from a shell and tube heat exchanger are not sufficient to maintain economical expectations.[10] A typical design of a helical-coil heat exchanger can be seen in figure 2.9.

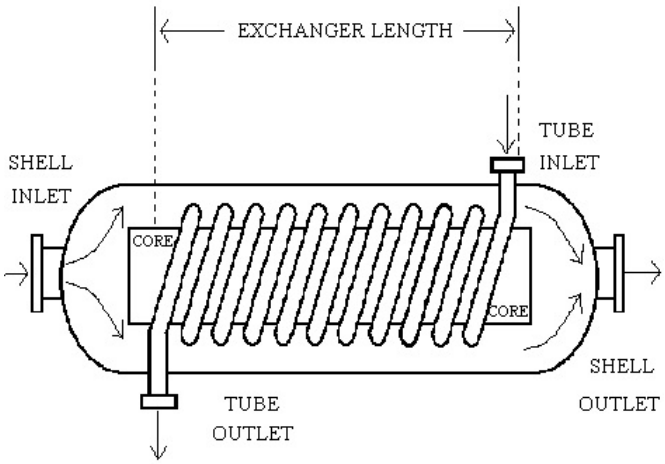

Figure 2.9: *Helical-cooil heat exchanger as designed by Scott S. Haraburda. Distributed under a CC-BY-SA 4.0 license.*

2.3.3 Heat transfer in heat exchangers

Heat transfer can occur in different ways which is termed different modes of heat transfer. As described in section **??** heat is transferred either through convection, conduction or radiation. These modes of heat transfer will only be covered briefly as described by Incropera et al.[8], which can be recommended for the interested reader. Heat transfer between a solid and a fluid through convection can be described as

$$q'' = \alpha(T_s - T_\infty)[W/m^2] \tag{2.8}$$

where T_s is the surface temperature, T_∞ is the fluid's free stream temperature and α is the convective heat transfer coefficient.

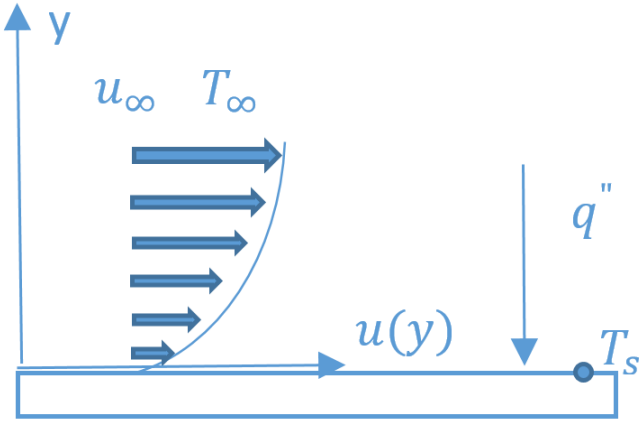

Figure 2.10: *Convection heat transfer between a fluid and a solid.*

In figure 2.10 the heat transfer between a fluid and a solid is visualized. If $T_s < T_\infty$ the heat flux q'' is transferred from the fluid to the plate. Conversely if $T_s > T_\infty$ the heat heat flux q'' is transferred from the plate to the fluid. The second mode of heat transfer that has to be considered is the conduction through the plate, which can be described by Fourier's law as

$$q'' = k\frac{T_{w,h} - T_{w,c}}{L} \quad \left[\frac{W}{m^2}\right] \tag{2.9}$$

where k is the thermal conductivity of the wall material and L is the distance the heat is transferred. The third mode of heat transfer, namely radiation, will not be considered further in this work but for the sake of convenience the heat flux from a body can be described as

$$E = \epsilon\sigma T_s^4 \tag{2.10}$$

where σ is Stefan Boltzmann constant and ϵ is called the emissivity, which is the proportion of how emissive the surface is compared to the ideal case of a black body.

2.3.4 Boiling heat transfer

In a Rankine system it is of utmost importance to correctly describe the two-phase flow in the boiler in order to predict the steam quality and flow available for the expander. Whereas theory only make difference between laminar and turbulent flow in one phase flow, things get more complicated in two phase flow as either phase can be laminar or turbulent and on top of that the two phases can be distributed differently in the flow. The two main types of boiling are pool boiling and flow boiling, in which a moving fluid is flowing through a heated tube or channel. Here the latter will be considered as it is the form of boiling relevant in a Rankine system, where there indeed is a flow. The main goal of engineering applications for boiling is usually to model the two-phase heat transfer coefficient which is written as

$$\alpha_{tp} = \frac{q}{\Delta T_e} = \frac{q}{T_{wall} - T_{sat}} \tag{2.11}$$

As the fluid is flowing through the tube at some critical heat flux, q''_{crit}, the onset of boiling occurs. This heat flux is reached at an instance, where the convective heat transfer is no longer enough to prevent the wall temperature from rising above the saturation temperature, T_{sat}. This occurs at $\Delta T_e = 5K$. [8]

In most two-phase models the heat transfer coefficients is modeled as a combination between the nucleate boiling- and the convective boiling heat transfer coefficient. Nucleate boiling is important for high heat flux rates whereas convective boiling is more dependent on mass flux and the steam quality, x. The heat transfer coefficient for two-phase flows can be modeled through superposition as

$$\alpha_{tp} = \left(h_{nb}^n + h_{cb}^n\right)^{\frac{1}{n}} \tag{2.12}$$

where α_{nb} and α_{cb} are the nucleate- and convective boiling heat transfer coefficients respectively. [11]

2.3.5 Expansion device

This component converts heat power to mechanical work by expanding the superheated steam through an expander, creating work as the enthalpy and pressure decreases. Using the notation in figure 2.4 the work output can be calulated as

$$\frac{\dot{W}_{exp}}{\dot{m}} = h_3 - h_4 \tag{2.13}$$

Expanders can roughly be divided into turbines which continuously does work while rotating and positive displacement machines, where the fluid is forced into a chamber changing the volume of the device. For small scale waste heat recovery systems the positive displacement machines are preferred, due to their lower rotation speeds and ability to operate under large pressure ratios[12]. Lower rotation speed are especially important for automotive applications as the much higher rotation speeds of turbines would lead to excessive gear ratios between the expander and motor.

2.3.6 Condenser

The condenser is used to convert the evaporated fluid into saturated liquid, in other words a phase transformation by cooling the working fluid below saturation temperature. [13].

2.3.7 Fluids

One of the most crucial questions for the integration of a Rankine cycle in an engine is the choice of a suitable working medium. The influence of working mediums are very important when it comes to Rankine cycles and its efficiency[14, pp.35-67]. Different working mediums like, water, ethanol, aceton and cyclopentane has their advantages and disadvantages. The working medium need to have proper thermodynamic properties as well as having to withstand the highly variable temperatures occurring in a motor without risk of freezing or hazardous risk of fire [15]. The maximum temperature and pressure in the cycle is also crucial to achieve a high efficiency. Studies of piston expanders with different working fluids has been done and it was shown that ethanol is the most favorable choice [16].

3

Methodology

In this chapter the methodology for the modeling of the Rankine system will be presented. All the equations used to model the components in SIMULINK and modeling assumptions are stated. The chapter will also give a brief introduction to the fluid library CoolProp that was used to retrieve fluid properties needed for the modelling.

3.1 CoolProp

CoolProp is a $C++$ library that calculates thermodynamic properties of pure fluids and mixtures. The fluid models implemented in CoolProp are based on Helmholtz energy formulation[17]. The library has been used to obtain fluid properties for ethanol and air. CoolProp calculates the state, for example enthalpy or entropy, for two given state variables, for example temperature and pressure. The library can also be used to obtain a state variable with inputs of one state and one state variable. The CoolProp library is implemented in the SIMULINK model for continuous calculations of enthalpies, pressures, temperatures, specific heats and other thermodynamic properties.

3.2 Expander

The expander will have a pressure ratio $r = 1 : 10$ which gives the pressure after the expander P_{out} as.

$$P_{in}r = P_{out} \tag{3.1}$$

By assuming isentropic expansion the isentropic enthalpy, $h_{2,is}$, after the expansion can be calculated from CoolProp from the outlet pressure, P_{out}, and the constant entropy, $s_1 = s_2$, obtained from the inlet temperature and pressure. The work produced by the expander can then be calculated by equation (3.2).

$$\dot{W}_{shaft} = \dot{m}(h_1 - h_{2,is})\eta_{is} \tag{3.2}$$

Where h_1 is the enthalpy before the expander and η_{is} is the isentropic efficiency obtained through interpolation from a map with inputs in form of pressure after the expander and the given expander speed σ (rpm).

The expander can only absorb a certain mass flow depending on different parameters, like rotation speed σ, volumetric efficiency η_{vol} and expander displacement volume V_d. The volumetric flow $\dot{V}$ are calculated by equation (3.3).

$$\dot{V} = \eta_{vol}\sigma V_d \tag{3.3}$$

Equation (3.3) together with the ideal gas law, makes it possible to calculate the mass flow through the expander $\dot{m}_{new}$. The new mass flow will be used to obtain the electrical pump power and to calculate the system pressure.

$$\dot{m}_{new} = \frac{\dot{V}P_{in}M}{RT_{in}} \tag{3.4}$$

Where M is the molar mass for ethanol, R the individual gas constant and T_{in} the temperature before the expander. The assumption of an ideal gas is usually valid for low pressures and high temperature. The compressibility factor is a measure of how far from an ideal gas a substance is, having the value 1 for a perfectly ideal gas. The compressibility factor for different degree of superheat can be seen in figure 3.1

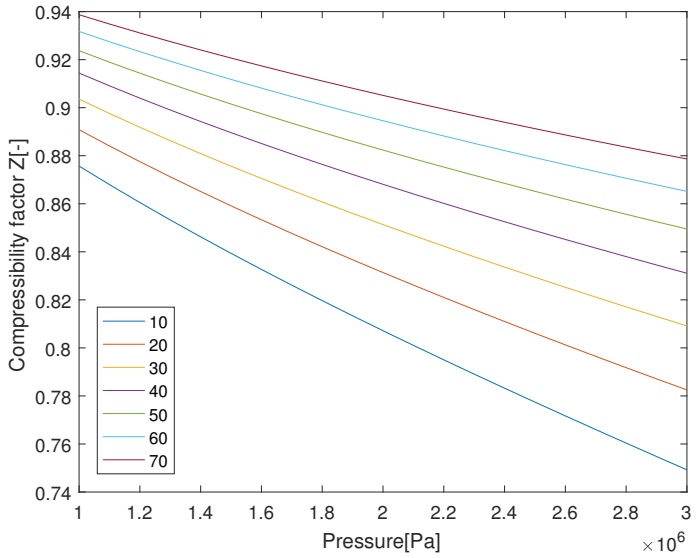

Figure 3.1: *The compressibility factor as a function of pressure for different levels of superheat*

As can be seen the assumption of an ideal gas will give some errors, but the error reduces with lower pressures and higher temperatures.

The pressure difference can now be calculated by taking the difference between the steam mass flow $\dot{m}_{hx}$ from the boiler into the expander and the mass flow m_{new} out of the system.

$$\Delta P = \frac{(\dot{m}_{hx} - \dot{m}_{new})RT_{in}}{V_{vap}} \tag{3.5}$$

Where V_{vap} is the volume occupied by the superheated steam, assuming small volume changes and thereby letting it be constant. The pressure difference ΔP can now be added to the old pressure P_{in} to obtain the new system pressure P_{sys}.

$$P_{sys} = P_{in} + \Delta P \tag{3.6}$$

3.3 Condenser

The evaporated mass flow must be condensed to saturated liquid because it is most energy efficient to compress a liquid. The working fluid travels through the condenser where latent heat is rejected at constant pressure. It is assumed that infinite cooling medium is available and the component is simply modeled as

$$\begin{aligned} h_{sat} &= h(P_{sat}) \\ T_{sat} &= T(P_{sat}) \end{aligned} \tag{3.7}$$

where h_{sat} and T_{sat} are the saturation enthalpy and temperature obtained with the help of CoolProp. Ideal is that the fluid expands to vapor saturation conditions in the expander. This is not always the case and it is assumed that both surplus sensible heat and the latent heat is cooled away in the condenser. It would have been possible to use the surplus sensible heat in a recuperator to preheat the fluid before entering the boiler.

3.4 Pump

The pump is the device that adiabatically compress the working fluid. The pressure itself is decided by the system inputs and the power input to the pump is the only variable that is controlled. By calculating the specific pump work W_{spw}, and knowing

the electrical efficiency makes it possible to obtain the electrical pump power W_{elec} required for a certain mass flow and system pressure.

$$W_{spw} = \frac{P_2 - P_1}{\rho \eta_{hydro}} \tag{3.8}$$

Where ρ is the density of the working fluid calculated in CoolProp from the inlet conditions. For an incompressible fluid the density is assumed constant. P_2 is the pressure after the pump and P_1 before the pump. The hydrodynamic efficiency η_{hydro} has been estimated to be 75% and the electrical pump power W_{elec} can be calculated by multiplying the mass flow $\dot{m}$ and divide it by the electrical efficiency η_{elec} that has been apporximated to be 85%.

$$W_{elec} = \frac{\dot{m}_{new} W_{spw}}{\eta_{elec}} \tag{3.9}$$

In this model the electrical pump power will be an output signal given by the system pressure and the new mass flow $\dot{m}_{new}$ calculated in the expander.

3.5 Boiler

Proper modelling of the heat transfer in a Rankine system is crucial to estimate the thermal efficiency of the model. The modelling of the two-phase heat transfer as well as the dynamic behavior that the transient wall conduction gives rise to, offer several challenges. The model is based on the basic conservation equations and has been discretized in the flow direction using the finite volume method.

3.5.1 Governing transport equations

The model of the heat exchanger is based on the conservation equations for mass, momentum and energy with several simplifications applied. The physical principle behind the continuity equation is that mass can be neither created nor destroyed. The continuity equation applied to a control volume fixed in space becomes

$$-\iint_A \rho \boldsymbol{V} dA = \frac{\partial}{\partial t} \rho d\mathscr{V} \tag{3.10}$$

and for one-dimensional steady state flow with constant cross section area, equation 3.10 can be rewritten as

$$\rho_{in} u_{in} A = \rho_{out} u_{out} A = \dot{m}_{in} = \dot{m}_{out} = \dot{m} \tag{3.11}$$

where u is the velocity component in the flow direction.

Conservation of momentum is based on Newton's second law of motion and for a one-dimensional steady state flow, the control volume formulation is written as

$$P_{in} + \rho_{in} u_{in}^2 = P_{out} + \rho_{out} u_{out}^2 \tag{3.12}$$

assuming that the boiler is isobaric, equation 3.12 simplifies to

$$\rho_{in} u_{in}^2 = \rho_{out} u_{out}^2 \tag{3.13}$$

Finally the control volume formulation for the energy equation, which is based on the first law of thermodynamics, is written as

$$\dot{E} = \dot{Q} - \dot{W}_{shaft} + \dot{m}_{in}\Big(h_{in} + \frac{u_{in}^2}{2} + g z_{in}\Big) - \dot{m}_{out}\Big(h_{out} + \frac{u_{out}^2}{2} + g z_{out}\Big) \tag{3.14}$$

which with previous simplifications, neglection of the potential energy potential, $g(z_{in} - z_{out}) = 0$, and zero internal heat gains, $\dot{Q} = 0$, simply writes

$$\dot{E} = \dot{m}(h_{in} - h_{out}) \tag{3.15}$$

3.5.2 Heat transfer equations and modelling assumptions

The heat transfer considered in the model is convection from the hot fluid to the colder tube and outer walls, conduction through the walls, and convection from hot walls to colder fluids.

3.5.3 Hot side heat transfer equations

The heat transfer considered for the hot side of the control volume is convection from the hot fluid to the colder tube and the surrounding walls. The convection is described as

$$\dot{q}_{h,w} = \alpha_h(\overline{T}_h - T_{h,w}) dA_{h,w} \tag{3.16}$$

where $dA_{h,w}$ is an area element of the tube wall. α_h is the heat transfer coefficient on the hot side and can be calculated as

$$\alpha_h = \frac{Nu_D k_h}{D_h} \tag{3.17}$$

where Nu_D is the Nusselt number, D_h is the outside tube diameter and k_h is the conductivity for the fluid on the hot side. The Nusselt's number has been calculated using an empirical equation from Hilpert[18]

$$Nu_D = CRe_D^m Pr^{\frac{1}{3}} \tag{3.18}$$

where Re is the Reynold's number, $Re = \frac{\rho u D_h}{\mu}$, μ_c is the fluid's dynamic viscosity and μ_s is the wall viscosity. The Prandtl number is defined as, $Pr = \frac{C_p \mu_c}{k_h}$. The constants m and c is dependent on the Reynold's number. The heat transported by the fluid into and out of the control volume is described by

$$\dot{q}_h = \dot{m}_h(h_{h,in} - h_{h,out}) \tag{3.19}$$

3.5.4 Cold side heat transfer equations

The heat transfer considered for the hot side of the control volume is convection from the hotter tube wall to the fluid. The convection is described as

$$\dot{q} = h_c(T_{w,c} - \overline{T}_c)dA_{c,w} \tag{3.20}$$

where the heat transfer coefficient α_c can be calculated as

$$\alpha_c = \frac{Nu_D k_c}{D_h} \tag{3.21}$$

where N_D is the Nusselt's number and k_c is the conductivity for the fluid on the cold side. The Nusselt's number has been calculated using the Sieder-Tate correlation

$$Nu_D = 0.027 Re_D^{\frac{4}{5}} Pr^{\frac{1}{3}} \left(\frac{\mu_c}{\mu_s}\right)^{0.14} \tag{3.22}$$

where D is the inside tube diameter, Re the Reynold's number, $Re = \frac{\rho u D}{\mu}$, μ_c is the fluid's dynamic viscosity and μ_s is the wall viscosity. The Prandtl number is defined

as, $Pr = \frac{C_p \mu_c}{k}$. The heat transported by the fluid into and out of the control volume is described by

$$\dot{q}_c = \dot{m}_c(h_{c,in} - h_{c,out}) \tag{3.23}$$

3.5.5 Two-phase modeling

When the enthalpy of the ethanol reaches the saturation point, h_l, the Sieder-Tate relation is not valid anymore. For the range where $h_l \leq h \leq h_v$ the relations proposed by Klimenko have been used[19]. For this two-phase model a convective boiling number, N_{CB} is defined as

$$N_{CB} = G\Big(\frac{h_{vap}}{q''}\Big)\Big[1 + x\Big(1 + \frac{\rho_l}{\rho_v} - 1\Big)\Big]\Big(\frac{\rho_v}{\rho_l}\Big)^{\frac{1}{3}} \tag{3.24}$$

where x is the mass fraction of vapor, ρ_l is the density at the liquid saturation point, ρ_v is the density at the dew point, h_{vap} is the heat of vaporization and G is the mass flux. If $N_{CB} \leq 1.6x10^4$ nucleate boiling is dominant and if $N_{CB} \geq 1.6x10^4$ the heat transfer is more dependent on forced evaporation. The heat transfer for respective case is

$$\begin{aligned}
&\alpha_{nucl} = 6.8x10^{-3} Pe_m^{0.6} Pr_l^{-0.33}\Big(\frac{Pb}{\sigma}\Big) \\
&\text{for} \quad N_{CB} \leq 1.6x10^4 \\
&\alpha_{fc} = 0.087 Re_m^{0.6} Pr_l^{\frac{1}{6}}\Big(\frac{\rho_v}{\rho_l}\Big)^{0.2} \\
&\text{for} \quad N_{CB} \geq 1.6x10^4 \\
&\text{where} \\
&Pe_m \equiv \frac{q'' b \rho_l c_{p,l}}{h_{vap}\rho_v k_l} \quad \text{is the modified Peclet number} \\
&Re_m \equiv G\Big[1 + x\Big(\frac{\rho_l}{\rho_v} - 1\Big)\Big]\frac{b}{\mu_l} \quad \text{is the modified Reynold's number} \\
&b \equiv \sqrt{\frac{\sigma}{g(\rho_l - \rho_v)}} \quad \text{is the Laplace constant}
\end{aligned} \tag{3.25}$$

3.5.6 Heat transfer through the walls

The heat transfer through a tube is described by Fourier's law of conduction

$$\dot{q}_w = \frac{(T_{h,w} - T_{c,w})2\pi k_{steel} dL}{ln\left(\frac{r_h}{r_i}\right)} \tag{3.26}$$

The heat loss to the ambient is described in the same way, with the difference that the outer wall is divided into two parts, the first one in steel and the second one made up of insulation material.

$$\dot{q}_w = \frac{(T_{h,w} - T_{c,w})2\pi k_{steel}}{ln\left(\frac{r_h}{r_i}\right)} \tag{3.27}$$

3.5.7 Heat balance for a control volume

The equations describing the heat balance for one volume segment of the heat exchanger can be derived from figure 3.2 and figure 3.3.

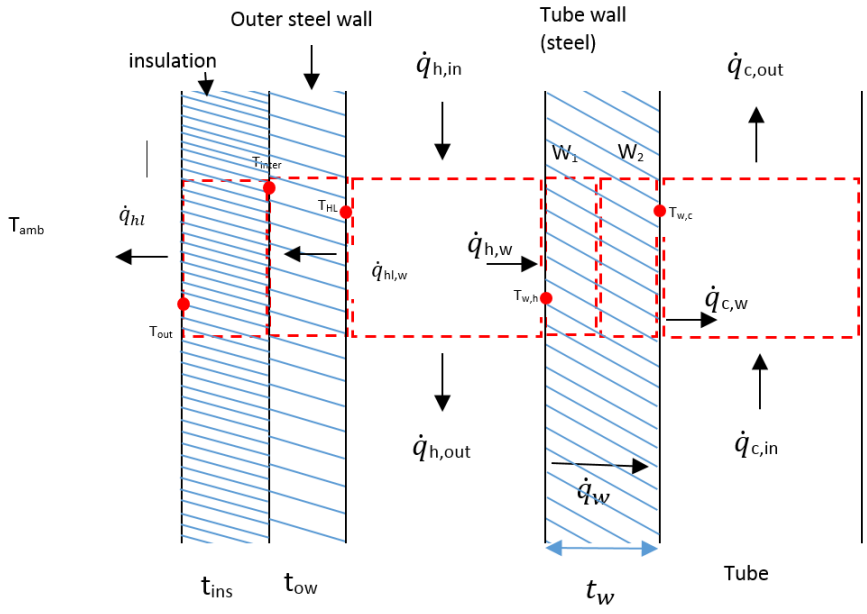

Figure 3.2: *Heat balance for a finite volume element of the heat exchanger. The control volume can be divided into subelements that give rise to a set of coupled ordinary differential equations.*

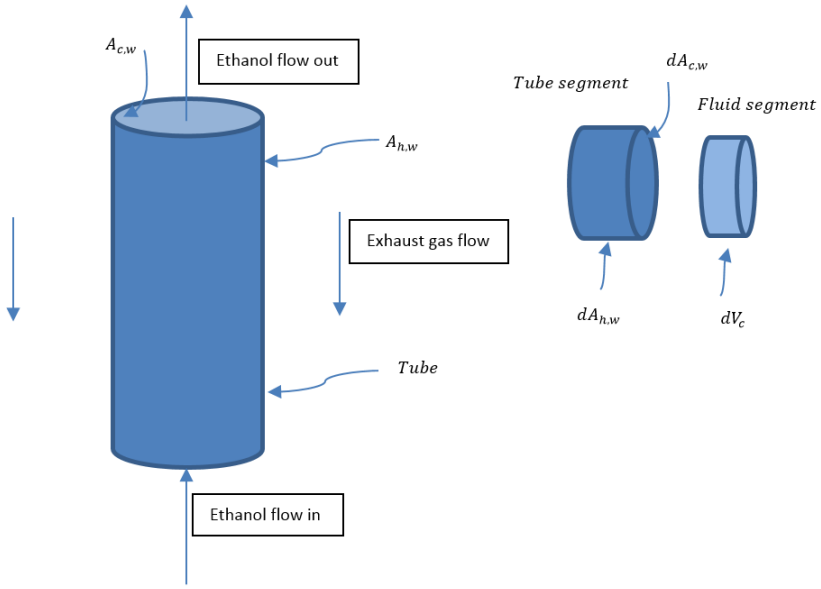

Figure 3.3: *Notations for a finite volume element of the heat exchanger.*

Several simplifications and assumptions have been applied to the model which include

- For simplicity the effects of wall conduction in the axial direction have been neglected. However several authors have concluded that there will be a conductive heat flow in the wall opposite to the fluid's flow direction.[20][21].
- Spatial discretization of the boiler into N elements in axial direction.
- Neglecting the dispersive and conductive heat transfer in the axial direction. This is true for clearlys turbulent flows with high Peclet number, $Pe > 55$[22].
- Isobaric heat transfer.
- Modeling of the tube wall in two parts in order to get the wall temperatures.
- Neglecting the effects of fouling.
- Neglecting the effects of radiative heat transfer. The effects of radiative heat transfer are small compared to other modes of heat transfer. This has been concluded in a study where the impact of radiative heat transfer in cross flow tube heat exchangers were calculated to a relative difference of less than 2%. [23]
- Mean properties given from CoolProp library as $\rho(P, \frac{T_{in}+T_{out}}{2})$, $\mu(P, \frac{T_{in}+T_{out}}{2})$ etc.

With stated assumptions and simplifications the heat transfer for the whole control

volume can be written. Starting with the hot fluid channel with exhaust gas:

$$\overline{\rho}_h \overline{c}_{p,h} dV_h \frac{dTh_{out}}{dt} = \dot{q}_{h,in} - \dot{q}_{c,in} - \dot{q}_{hl,w} - \dot{q}_{h,w} = \dot{m}_h (c_{p,} T_{h,in} - c_{p,h} T_{h,in}) - \dot{q}_{hl,w} - \dot{q}_{h,w} \tag{3.28}$$

where

$$\dot{q}_{h,w} = (\overline{T}_h - T_{w,h}) \alpha_h A_h \tag{3.29}$$

is the heat entering the tube wall and

$$\dot{q}_{hl,w} = (\overline{T}_h - T_{hl}) \alpha_h A_{h,outer} \tag{3.30}$$

is the heat loss to the ambient.

And for the cold fluid channel with ethanol flow the heat balance is

$$\overline{\rho_c} dV_c \frac{dh_{c,out}}{dt} = \dot{q}_{c,in} - \dot{q}_{c,out} + \dot{q}_{c,w} = \dot{m}_c (h_{c,in} - h_{c,out}) + \dot{q}_{c,w} \tag{3.31}$$

where

$$\dot{q}_{c,w} = (T_{w,h} - \overline{T}_c) \alpha_c A_c \tag{3.32}$$

is the heat entering the cold side control volume. Further the control volume for the separating tube wall follows, starting with the first wall segment(w1)

$$A_1 \frac{t_w}{2} \rho_w c_{p,w} \frac{dT_{w,h}}{dt} = \dot{q}_{h,w} - \dot{q}_w \tag{3.33}$$

and the second wall segment w2

$$A_2 \frac{t_w}{2} \rho_w c_{p,w} \frac{dT_{w,c}}{dt} = \dot{q}_w - \dot{q}_{c,w} \tag{3.34}$$

where

$$\dot{q}_w = (T_{w,h} - T_{c,w}) \frac{k_w 2\pi dL}{ln\left(\frac{r_o}{r_i}\right)} \tag{3.35}$$

Is the heat transferred through the wall. Finally the heat loss through the outer wall that is divided into three parts can be described by the following set of equations. First part of the wall that is constructed of steel

$$A_{ow}t_{ow}\rho_w c_{p,w}\frac{dT_{hl}}{dt} = \dot{q}_{hl,w} - (T_{hl} - T_{ins})\frac{k_w 2\pi dL}{ln\left(\frac{r_{ow}}{r_{iw}}\right)} \tag{3.36}$$

The second part of the wall that is an insulation material

$$A_{ins}t_{ins}\rho_{ins}cp_{ins}\frac{dT_{hl}}{dt} = (T_{hl} - T_{ins})\frac{k_w 2\pi dL}{ln\left(\frac{r_{ow}}{r_{iw}}\right)} - (T_{ins} - T_{out})\frac{k_{ins}2\pi dL}{ln\left(\frac{r_{o,ins}}{r_{i,ins}}\right)} \tag{3.37}$$

and lastly the tiny wall control volume

$$A_{ins,o}t_{ins,o}\rho_{ins}cp_{ins}\frac{dT_{out}}{dt} = (T_{ins} - T_{out})\frac{k_{ins}2\pi dL}{ln\left(\frac{r_{o,ins}}{r_{i,ins}}\right)} - Q_{hl} \tag{3.38}$$

where $\dot{q}_{hl}$ is the heat admitted to the ambient

$$\dot{q}_{hl} = (T_{out} - T_{amb})\alpha_{out}A_{out} \tag{3.39}$$

3.5.8 Spatial discretization

The boiler have been discretized in axial direction using the finite volume method with limited discretization, N. The spatial discretization scheme used is the bounded central differencing scheme, which uses mean values to calculate the present value of some property Φ.

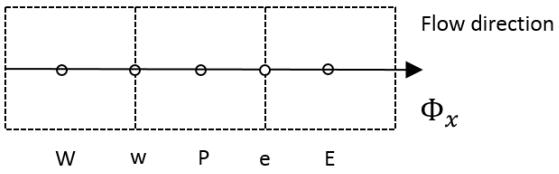

Figure 3.4: *The central differencing scheme is known to be robust due to that its boundedness.*

The grid that was set up is uniform in the flow direction (Fig.3.4) and the properties Φ is calculated as given in equation 3.40.

$$\Phi_e = \frac{\Phi_P + \Phi_E}{2}$$
$$\Phi_w = \frac{\Phi_W + \Phi_P}{2} \tag{3.40}$$

3.5.9 Setup in Simulink

A schematic of the discretization made to the boiler can be seen in (Fig.3.5).

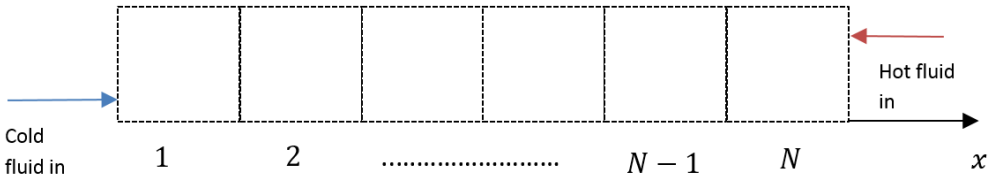

Figure 3.5: *The boiler is discretized and divided into N elements.*

The set of ordinary equations derived in section 3.5.7 are solved for the whole heat exchanger volume that is discretized in both space and time, a so called temporal discretization. This gives rise to the initial value problem

$$\frac{\partial \Phi}{\partial t}(x,t) = F(t,\Phi) \quad t[t_0, t_f], \quad \Phi(t_0) = \Phi_0 \tag{3.41}$$

which was solved in SIMULINK with the help of the ODE45 solver. The ODE45 is a based on the Dormand-Prince principle, which is a theoretical refinement of the Runga-Kutta method. [24]

3.5.10 Boiler (Simplified)

The simplified boiler were constructed due to that the original boiler performed to slow when it was integrated in the Rankine cycle. The component was modeled by using maps with calculated data of steam mass flows $\dot{m}_{hx}$ and steam temperatures for a given system pressure and exhaust heat power. The enthalpy after the boiler h_s can be obtained by using CoolProp (Fig.3.6).

The amount of stainless steel that covers the heat boiler stores a lot of heat energy, so a power delay of 15 seconds and a heat rate transfer of 85% will be used as parameters to obtain a more realistic system.

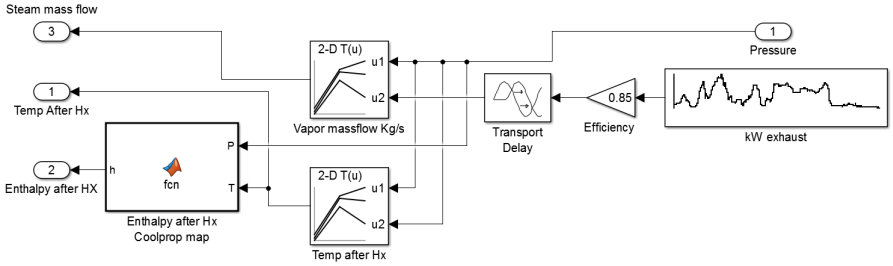

Figure 3.6: *Simplified boiler. The figure visualizes the SIMULINK construction and the different maps for temperature, steam mass flow (vapor) and the enthalpy from CoolProp after the boiler (simplified), hx = boiler.*

4

Results

In the following chapter the results for the whole model with the simplified boiler, as well as separate results for the discretized boiler will be presented. This division has been done because it turned out that the boiler were to slow to be practically used together with the other parts in the Rankine model.

4.1 Results for the whole system

Driving data has been collected by Volvo Cars in the form of exhaust gas temperatures, exhaust mass flows and engine speed for different vehicle speed. From this set of data the corresponding exhaust heat power has been calculated. The whole driving section where divided into three parts, based on different load cases. These parts where analyzed for different expander gear ratios to calculate the cycle's effectiveness. These measurements will give an indication of how the system operates and where it generates the best output. The first section, the yellow one in figure 4.1 represents the exhaust heat power corresponding to city driving, where the vehicle velocity is limited generating low engine speed and low exhaust heat power. The red and green area corresponds to data collected from driving on rural roads and highways respectively. Each simulation has its own simulation time that are listed in the different tables that presents the results. The results are presented in the form of mean values of energy put into the pump, expander energy output, system pressure, steam temperature, steam mass flow, heat power from exhaust gases and thermal efficiency. A simulation with constant heat power were made, to easily evaluate the functionality of the computational model (Fig. 4.4).

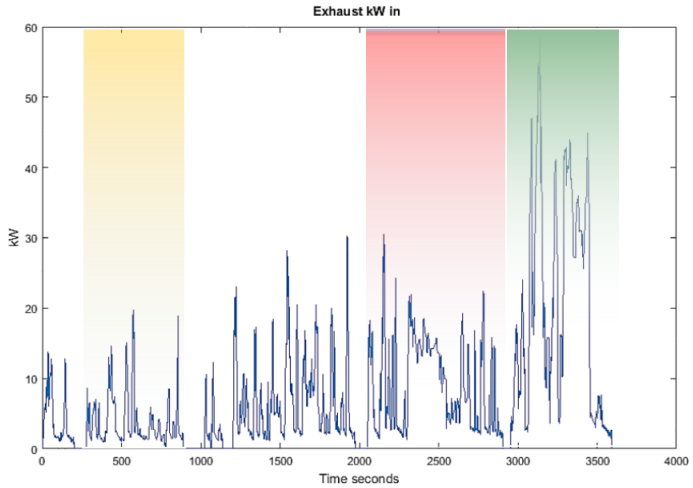

Figure 4.1: *Collected driving data representing the exhaust power into the system generated by the vehicle. Yellow region = city driving. Red region= rural roads. Green region = motorway driving.*

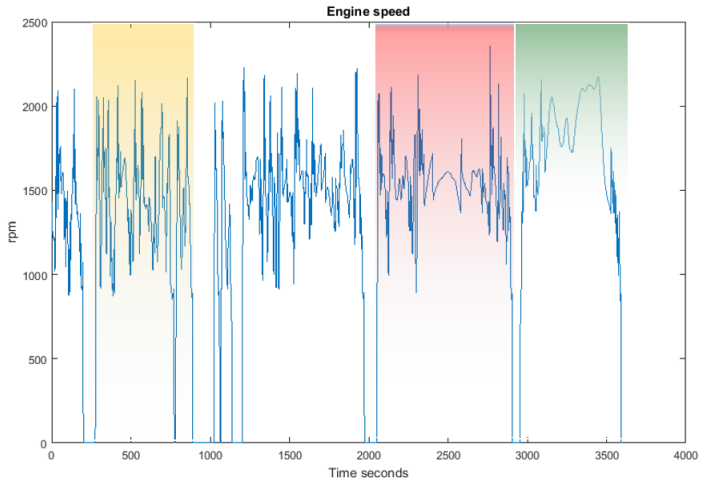

Figure 4.2: *Collected driving data representing the engine speed generated by the vehicle. Yellow region = city driving. Red region= rural roads. Green region = motorway driving.*

The simulations were run for gear ratios of 1:1, 1:1.5 and 1:2 and the results of each case are listed in data tables for analysis. Table 4.2 represents highway driving for the different gear ratios, table 4.3 belongs to city driving and table 4.4 to rural road driving.

The green area in figure 4.1 and 4.2 representing the highway driving could not be simulated. Engine speeds and exhaust heat power with such high frequencies were difficult for the model to evaluate and gave either unreasonable values or made the model crash. By building own signals in SIMULINK with engine speed and exhaust heat power levels corresponding to highway driving (Tab. 4.1) made it possible

to approximate some results of that region. The isentropic efficiency map did not have data for system pressures over 40 bar so a mean value of 49 % was used to approximate the computations in table 4.2.

Mean values	City	rural road	highway
Engine speed	1400 rpm	1500 rpm	1800 rpm
Heat power	4300 W	10000 W	24000 W

Table 4.1: *Mean values of engine speed and heat power put into the system obtained for three different driving fields; city, rural and motorway.*

Highway 300 seconds	Ratio 1:1	Ratio 1:1.5	Ratio 1:2
Pump energy in	26.85 kJ	21.35 kJ	—kJ
Expander Energy out	329.8 kJ	332.1 kJ	—kJ
System Pressure	29.6 bar	23.2 bar	—bar
Steam mass flow	13.4 g/s	13.5 g/s	— g/s
Steam Temperature	220°C	208°C	—°C
Exhaust energy in	$6.151 * 10^3$ kJ	$6.151 * 10^3$ kJ	$6.151 * 10^3$ kJ
Thermal efficiency	4.9%	5.0%	—%

Table 4.2: *Mean values of resulting system pressure, steam mass flow and steam temperature as well as total pump-, expander- and exhaust heat energies and the thermal efficiency of the system.*

City 500 seconds	Ratio 1:1	Ratio 1:1.5	Ratio 1:2
Pump energy in	3.354 kJ	2.879 kJ	2.837 kJ
Expander Energy out	63.35 kJ	59.57 kJ	45.51 kJ
System Pressure	7.7 bar	6.9 bar	6.3 bar
Steam mass flow	2.15 g/s	2.16 g/s	2.17 g/s
Steam Temperature	156°C	152°C	150°C
Exhaust energy in	$1.990 * 10^3$ kJ	$1.990 * 10^3$ kJ	$1.990 * 10^3$ kJ
Thermal efficiency	3.0%	2.9%	2.1%

Table 4.3: *Mean values of resulting system pressure, steam mass flow and steam temperature as well as total pump-, expander- and exhaust heat energies and the thermal efficiency of the system.*

Rural road 400 seconds	Ratio 1:1	Ratio 1:1.5	Ratio 1:2
Pump energy in	12.1 kJ	9.3 kJ	10.9 kJ
Expander Energy out	204 kJ	215 kJ	126 kJ
System Pressure	17.7 bar	14.8 bar	12.6 bar
Steam mass flow	6.7 g/s	6.8 g/s	6.8 g/s
Steam Temperature	194°C	181°C	176°C
Exhaust energy in	$4.098 * 10^3$ kJ	$4.098 * 10^3$ kJ	$4.098 * 10^3$ kJ
Thermal efficiency	4.7%	5.0%	2.8%

Table 4.4: *Mean values of resulting system pressure, steam mass flow and steam temperature as well as total pump-, expander- and exhaust heat energies and the thermal efficiency of the system.*

The figures below represents the results and behaviour of the different computed driving sections during different simulation times. Starting with a very small section (Figure 4.3) taken from the highway region and then with simulations representing the different colour regions from figure 4.2 and figure 4.1.

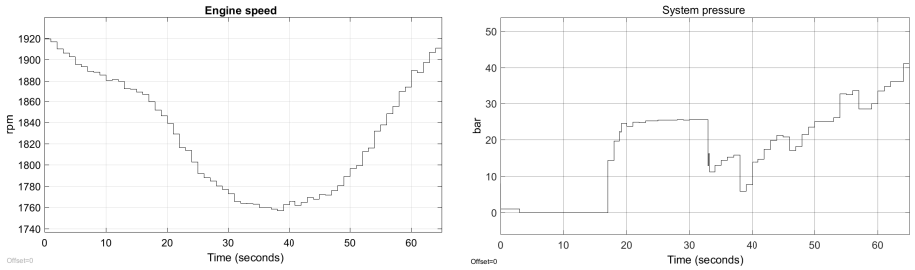

(a) Engine speed

(b) System pressure

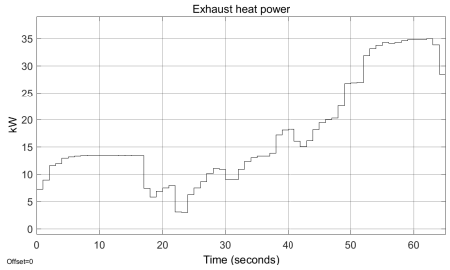

(c) Exhaust heat power in

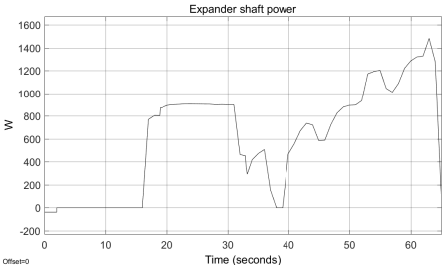

(d) Expander work out

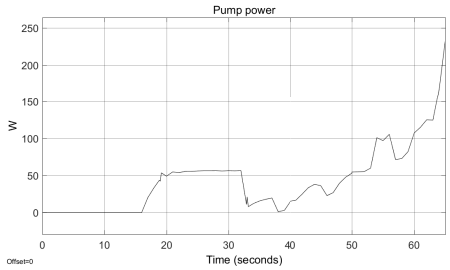

(e) Pump power in

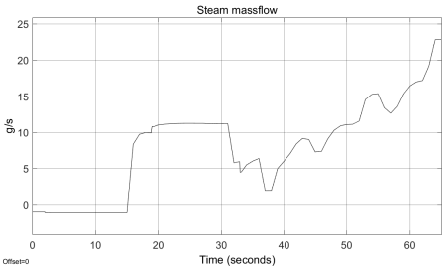

(f) Steam massflow

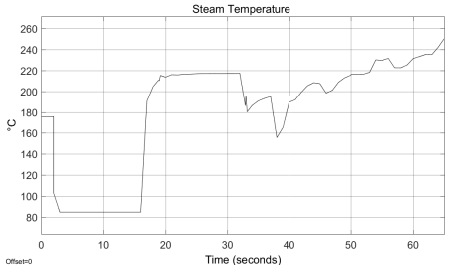

(g) Steam temperature

Figure 4.3: *Thermodynamic relations between engine speed and heat power put into the system. Engine speed taken from a very small section of the green region with a gear ration of 1:1 for 65 seconds.*

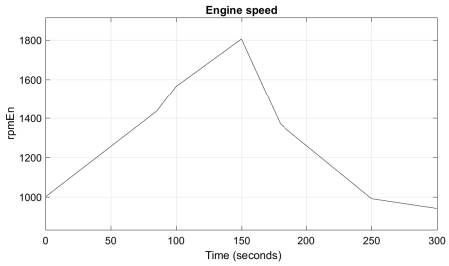

(a) Engine speed

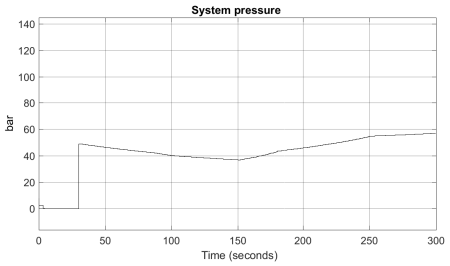

(b) System pressure

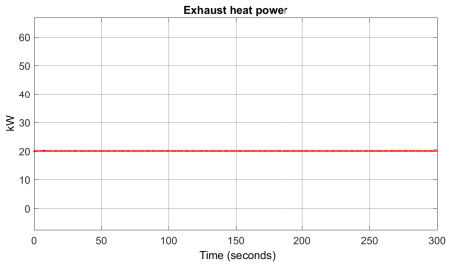

(c) Exhaust heat power in

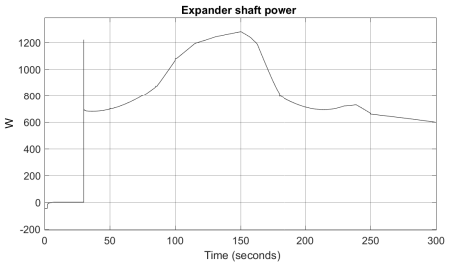

(d) Expander work out

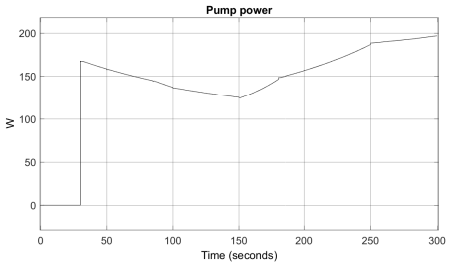

(e) Pump power in

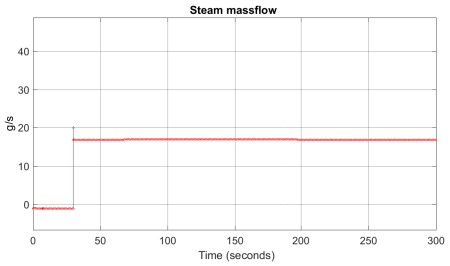

(f) Steam massflow

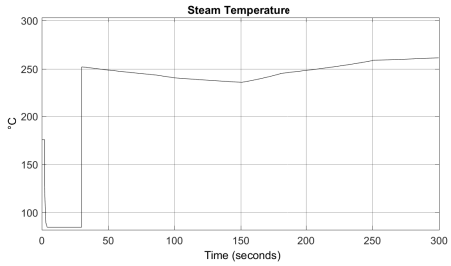

(g) Super heated steam temperature

Figure 4.4: *Thermodynamic relations between engine speed for a constant heat power input to the system.*

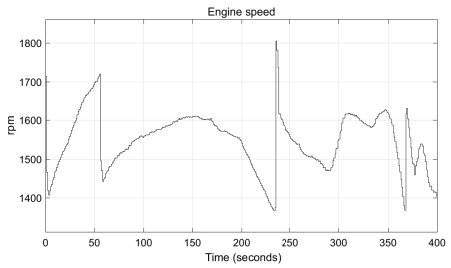

(a) Engine speed

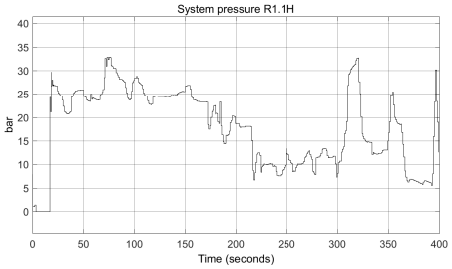

(b) System pressure

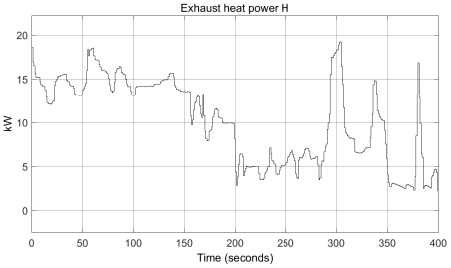

(c) Exhaust heat power in

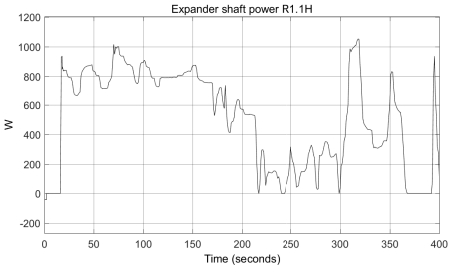

(d) Expander power out

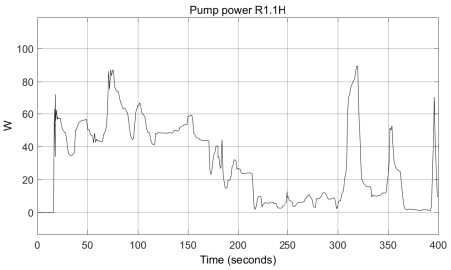

(e) Pump power in

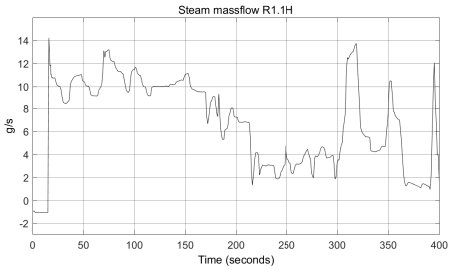

(f) Steam massflow

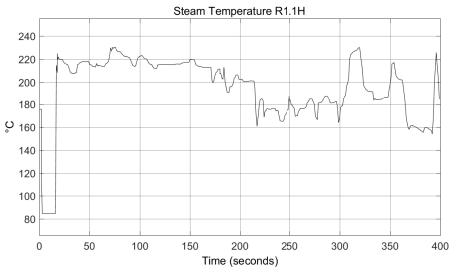

(g) Super heated steam temperature

Figure 4.5: *Thermodynamic relations between engine speed and heat power put into the system. Data collected from rural road driving. Gear ratio 1:1.*

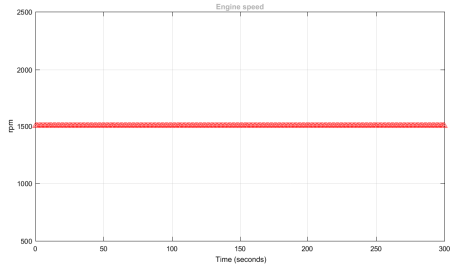

(a) Engine speed

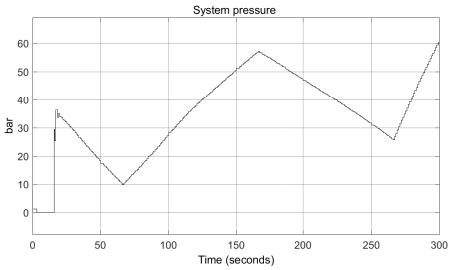

(b) System pressure

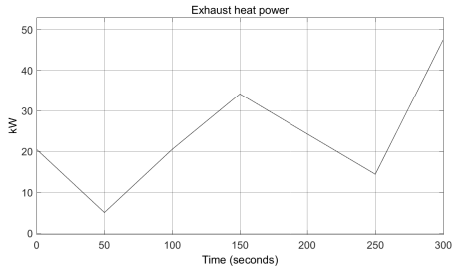

(c) Exhaust heat power in

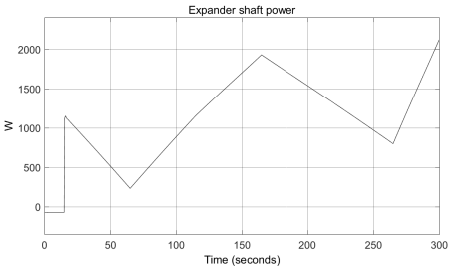

(d) Expander power out

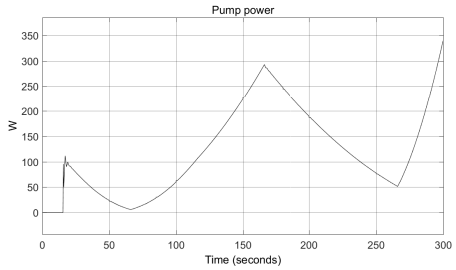

(e) Pump power in

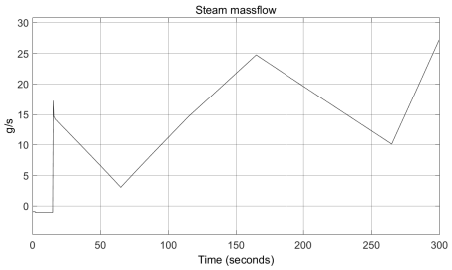

(f) Steam massflow

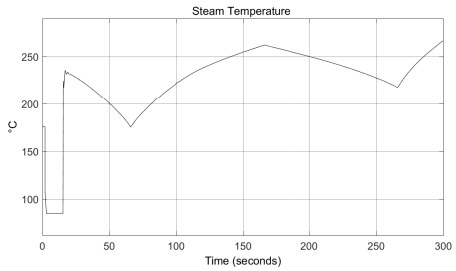

(g) Super heated steam temperature

Figure 4.6: *Thermodynamic relations between constant engine speed and varying heat power input to the system.*

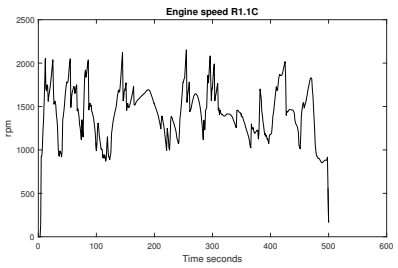

(a) Engine speed

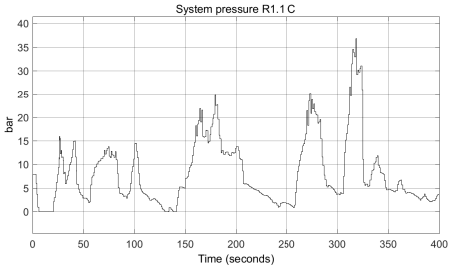

(b) System pressure

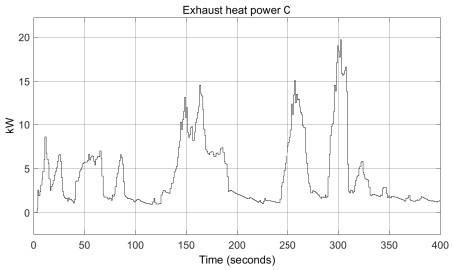

(c) Exhaust heat power in

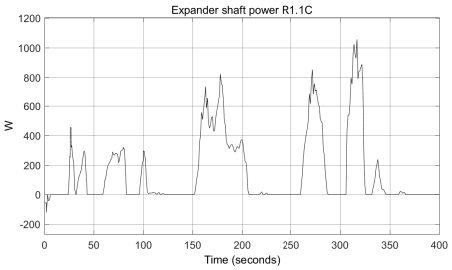

(d) Expander power out

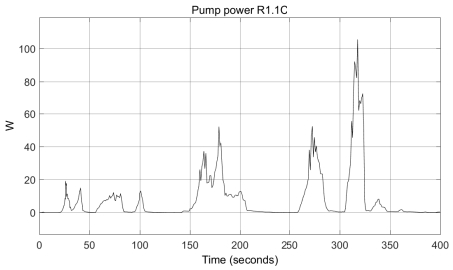

(e) Pump power in

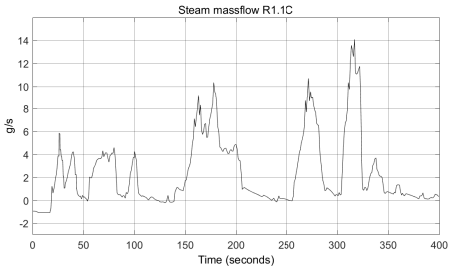

(f) Steam massflow

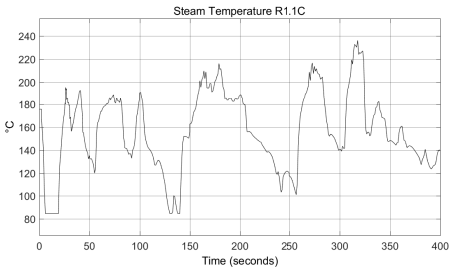

(g) Super heated steam temperature

Figure 4.7: *Thermodynamic relations between engine speed and heat power in to the system. Data collected from city driving. Gear ratio 1:1.*

4.1.1 Observations and discussion for the system results

The system pressure depends both on how much steam mass flow that can be produced for a given heat power from the exhaust gases and how the engine speed varies. Constant heat power input to the system and a decreasing engine speed will generate an increasing system pressure and vice verse. This is visualized in figure 4.4. This behaviours is also verified by figure 4.4 where the heat power is constant.

Since the expander has a geometric expansion of 1:10, the system will only operates for pressures above 10 bar, otherwise can the pressure go down under atmospheric pressure and generate air leak into the system. The waste heat recovery system will be bypassed for city driving since that region generates pressure below 10 bar 4.3.

The volumetric efficiency decreases with higher expander speed, which means that when the speed increases, the expander will have more complication to absorb the steam mass flow and that is why the system pressure and the expander speed are not linear 4.4.

Figure 4.3a represents the engine speed of a small section taken from the green region in figure 4.2. This section can be interpreted as a car breaking and accelerating on a highway during 60 seconds. A possible way to obtain a constant system pressure could be by having an increasing engine speed together with an increasing steam mass flow, assuming a proportional increasing behaviour between both parameters. The temperature for the working fluid should increase when the pressure increases at a constant heat input, which can be verified by figure 4.4g.

Even if the engine speed increases the last 30 seconds in figure 4.3a it does not necessarily mean that the pressure should drop. If the heat power input were constant this would be the case, but now the steam flow increases directly proportional to the heat power and faster than the engine speed, which results in a system pressure increase. The steam mass flow does not only depend on the exhaust heat power, but also on the system pressure so there is an evident dynamic behaviour in the system.

A constant engine speed (Figure 4.6a) and an increasing exhaust heat power (Figure 4.6c) will generate an increasing system pressure (Figure 4.6b) since higher heat power also means more steam mass flow. Figure 4.3c shows the exhaust heat power input to the system and the steam mass flow (Figure 4.3f) produced in the heat exchanger. Both charts shows a clear relation to each other having the same pattern. An increase in heat power will generate more steam mass flow and perhaps increase the system pressure, which can easily be seen by comparing figure 4.3f and figure 4.3b.

The thermal efficiency is higher for rural driving conditions and highways compared to city driving and the most efficient gear ratio is 1:1.5 for all cases except for the city driving that shows a decrease in thermal efficiency with ratio 1:1.5. Unfortunately the model was unable to perform simulations for highway data at a ratio of 1:2, but this can be assumed to be an ineffective ratio as it was for the other driving regions.

By increasing the gear ratio the system pressure will drop as shown in both table 4.4 and table 4.3. This is something that can be expected since an increase in expander speed will let more steam flow through the system, and due to that decrease the system pressure. The mean steam temperature are of course lower for city driving compared to rural roads and so is also the the steam mass flow. The mean engine speed is also lower but it does not mean that the system pressure always should be higher for a lower engine speed. The steam mass flow when driving on rural roads is much larger and that explains why the system pressure also is higher. It is a combination of both parameters as mentioned before.

The simplified boiler in the model has a delay of 15 seconds before the heat transfer starts to act. This means that the Rankine cycle does not start to do work until the boiler start to produce steam mass flow. The delay time can also explain the dead time at the beginning of all steam mass flow simulations.

There is a direct relation between the engine speed (Figure 4.4a) and the expander work output (Figure 4.4d), as a high engine speed means a large mass flow through the expander which leads to more power output. By comparing the pump curve, the system pressure and the engine speed behaviour, it can be concluded that a decreasing speed will increase the system pressure and to maintain that pressure the pump has to work at a higher power level.

4.2 Boiler

In this section the results of the discretized boiler will be presented. Results from steady state simulations, transient simulations and the effect of the discretization level will be covered.

4.2.1 Steady state simulation

The simulation was run for typical heat up conditions with a heat input, $\dot{q}_{ref} = \dot{m}_h c_{p,h}(T_{exh} - T_{amb}) = 35\ kW$. Other input variables can be seen in table 4.5

T_{exh}	T_{amb}	P_{exh}	P_c	P_{amb}	$\dot{m}_h$	$\dot{m}_c$
750[°C]	25[°C]	1.3 [bar]	25 [bar]	1.01325 [bar]	45 [g/s]	20[g/s]

Table 4.5: *Typical conditions that were used for steady state simulations.*

The resulting temperature leaving the boiler for the steady state simulation can be seen in figure 4.8.

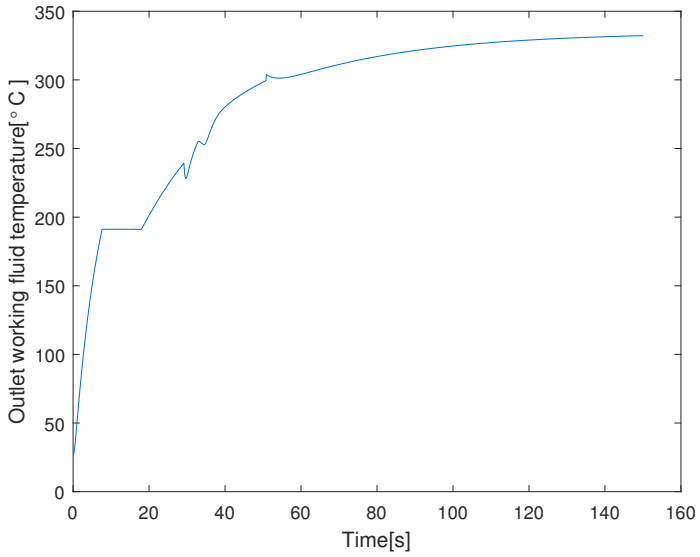

Figure 4.8: *Boiler tested for steady state heat up from ambient conditions. Discretization level N=20*

The results looks somehow realistic but there are some unexpected jumps in the steam temperature between 30 and 40 seconds and around 60 seconds possibly due to numerical error. In figure 4.9 the temperature variation along the axial direction in the boiler is visualized.

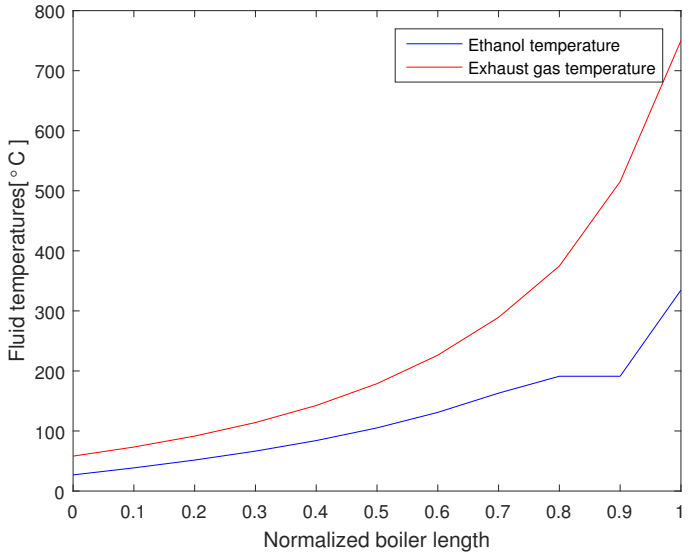

Figure 4.9: *Fluid temperature distribution over the normalized heat exchanger length.*

The effectiveness of the boiler can be calculated as

$$\epsilon = \frac{(h_{c,out} - h_{c,in})\dot{m}_c}{(T_{h,in} - T_{amb})\dot{m}_h c_{p,h}} = \frac{(1.34 * 10^6 - -1.36 * 10^5)20^{-3}}{(750 - 25)45 * 10^{-3}} = 0.695 = 69.5\% \quad (4.1)$$

In figure 4.10a and 4.10b the heat transfer coefficient for the ethanol side and the flue gas side respectively can be seen.

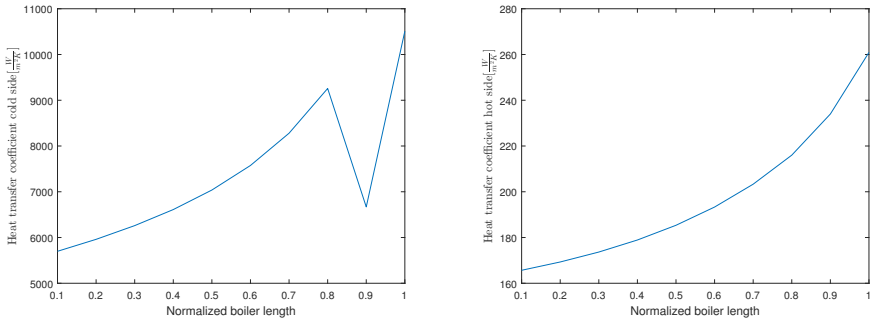

(a) *Heat transfer coefficient inside the tube*

(b) *Heat transfer coefficient for the external flow*

Figure 4.10: *Heat transfer coefficient for the internal as well as the external flow for N=10.*

The results of the temperature along the axial direction depicted in figure 4.10 were not exactly as could be unexpected. One can clearly see the three different phases for the ethanol flow; one phase liquid, two-phase and one phase gas. However the pinch point was expected to be closer to the liquid saturation point and a more linearly temperature distribution for the flue gas side was expected. But as can be seen the driving force for the heat transfer increases throughout the cold side's fluid flow direction. The heat transfer for the hot side is increasing throughout the heat exchanger's length and the cold side heat transfer coefficent is increasing until the start of the evaporator. Even though the temperature distribution correlates with its heat transfer coefficent the almost exponential shape of the curve seem a bit unrealistic. The decreasing heat transfer coefficient at the position where the boiling is initiated is also a bit unexpected as it was expected to increase in the two-phase region. The results clearly follows the heat transfer coefficient and a choice of different models would most likely show other results.

4.2.2 Effects of discretization

A discretization of the boiler in 20 segments can be seen in figure 4.11 and the result for a discretization in 50 cells i shown in 4.12, which can be compared with the previously shown pinch point analysis in 4.9. The study of the level of discretization supports the previously mentioned apprehension that the heat transfer seem to

be increasing to much along the axial direction. Especially the results from the discretization in 50 segments are uncertain. The driving force for heat transfer along the first 70% of the axial direction is non existent, while the last 30% of the axial distance sees a sharp change in both fluids' temperature. What causes these confusing results is hard to say, but it seems that the driving temperature is way to high in the last segments so that there is not much driving force left moving towards the cold fluid's inlet. The results of the simulation with discretization level 50, could possibly be due to that some settings were wrong. Otherwise it is hard to explain why the results for the discretization with 50 cell is completely different compared to the two other discretizations.

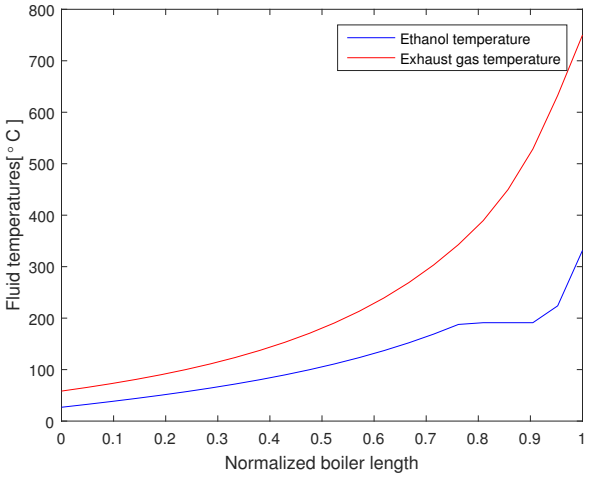

Figure 4.11: *Fluid temperature distribution for boiler divided into 20 segments.*

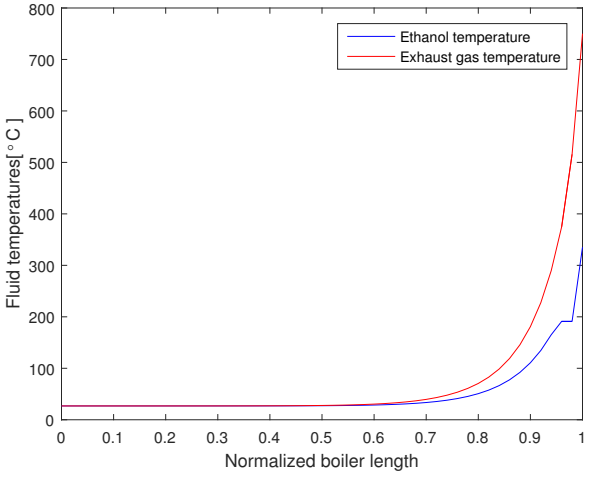

Figure 4.12: *Fluid temperature distribution for boiler divided into 50 cells.*

4.2.3 Transient simulation

The results of a transient simulation is plotted below in figure 4.13

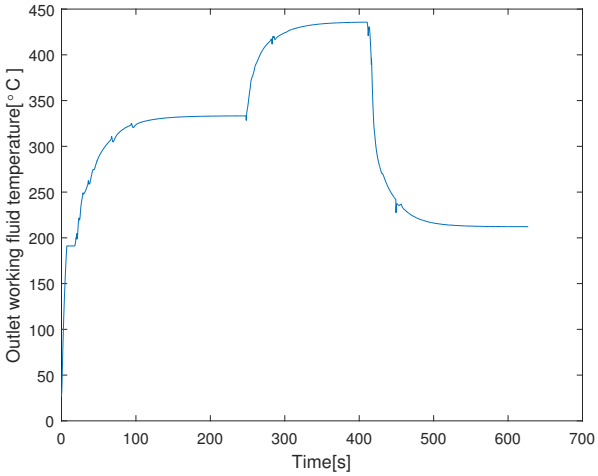

Figure 4.13: *Transient simulation with a step change in flue gas mass flow from 45 to 55 g/s at 250 seconds and from 55 to 35 at 420 seconds. The simulation is done with a discretization in 20 steps.*

As can be seen there is a delay in the temperature response of the ethanol fluid. This is because of the accumulation of heat in the walls and in the ethanol. As a comparison the simulation was run with 10 segments as well. The results are shown in figure 4.14.

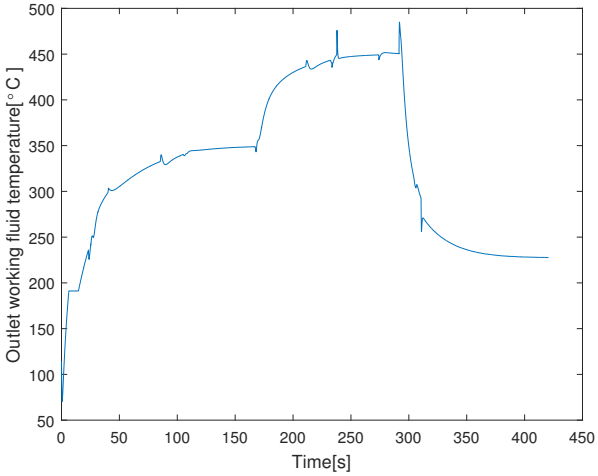

Figure 4.14: *Transient simulation with a step change in flue gas mass flow from 45 to 55 g/s and 55 to 35. The simulation is done with a discretization of 10 steps.*

Comparing the different discretization one can see that the results for the finer

discretization is much smoother, which probably is a cause of smaller changes in enthalpy per cell volume.

4.2.4 Computation time considerations

As mentioned in the beginning of the results section the heat exchanger model is much to slow to be practically implemented in the system model. A steady state simulation of a model divided into 10 steps takes approximately two days to run. This is mainly because of repeating call to the fluid's database CoolProp, which considerable slows up computations. Actions to speed up the model by using TTSE interpolation to calculate fluid properties would increase the speed per call 115 times[25]. Despite the efforts speeding up the code the Profiler Reporter in Simulink showed that the calls to CoolProp amounted to a total of 85% of the computational time.

5

Conclusion

It can be concluded that model based design in SIMULINK is well suited to simulate the behavior of a waste heat recovery system for passenger cars. Model based design is intuitive and cost effective and makes it possible to easily test the model for different driving scenarios. It should also be mentioned that the different components in the model could be easily switched to test similar components based on other technologies thanks to the model based approach. Model based design also makes it possible to easily integrate the model in larger car simulation models.

The results shows positive results for waste heat recovery. Efficiency gains ranging from 2.85% for city driving conditions to 5.02% for motorways were achieved, which could be translated into approximately equal fuel savings, disregarding the decrease in horse power due to the waste heat appliances. Although the results were satisfying one has to keep in mind that models always have flaws and cannot be totally trusted. Therefore rig tests has to be performed to verify the results achieved from the simulations. The efficiency gains are satisfying regarding environmental considerations but whether fuel savings can motivate the cost increase is more difficult to evaluate and would be a subject for a separate study.

The best choice of gear ratio was found to be 1:1.5 for city and motorway driving conditions and 1:1 for city driving. Another reason for a gear ratio of 1:1.5 is suitable is that the piston expander should not expand to sub atmospheric conditions due to the risk of air leaking into the system. For city driving conditions where the system pressure does not reach 10 the expander could be bypassed in favor of a turbine that can produce electric power.

Modeling a boiler was proved to be difficult but satisfying results were achieved for the component itself. However the computational time for the component were in excess of what is acceptable for a model of this type and integration of the component to the Rankine model was not possible due to this. A modeling approach with a dicretized unit which repeatedly called the fluid library CoolProp was the cause of the excessive computational times. Especially the calls to CoolProp were time consuming and accounted for 85% of the computational time. Efforts were made to integrate data from CoolProp in maps in SIMULINK but the nonlinearities associated with the two-phase flow regime made it difficult and gave and less accurate results.

Whatever path the automotive industry will follow in the future and whether waste heat recovery will be a part of it or not, time will tell.

6

Future work

There are several fields that future work could focus around. The model have some flaws that has to be dealt with. The model needs to be stable for higher expander revolution speeds and large deviations in revolution speed. It would be interesting as well to extend the model so that it works for system pressures below 10 bar with the expander bypassed and investigate if it is beneficial to generate electricity in this range.

The boiler model have to be looked into especially the slow compuational speed has to be dealt with. Ideas how this could be done is either by integrating the equations giving the state of the working fluid directly into SIMULINK, which probably would be difficult, or update the state of fluid properties less frequently in regions where changes are low. CFD simulations on the component would be interesting as well and results from such a model could possibly be used to set up a simpler heat exchanger model. The choice of two-phase model in the boiler could also be looked into, because proper description of evaporation is important to give a realistic model. Almost as important as the boiler is the condensing heat exchanger unit, because surplus heat must be removed although this sounds contradictory when the goal is to utilize as much heat as possible.

The pump and expander components could also be covered in more detail but the most urgent is definitely the heat exhanger.

Bibliography

[1] Yu, C., Chau, K.T. Thermoelectric automotive waste heat energy recovery using maximum power point tracking. Energy Conversion and Management. 2009;50(6):1506-1512.

[2] Sprouse III C., Depcik C. Review of organic Rankine cycles for internal combustion engine exhaust waste heat recovery. Applied Thermal Engineering. 2013;51(1-2):711-722.

[3] Cengel, Y.A., Boles, M.A. THERMODYNAMICS An Engineering Approach. Sixth Edition. New York: McGraw-Hill; 2007

[4] Wang, E.H., Zhang, H.G., Fan, B.Y., Ouyang, M.G., Zhao, Y., Mu, Q.H. Study of working fluid selection of organic Rankine cycle (ORC) for engine waste heat recovery. Energy. 2011;36(5):3406-3418

[5] Massoud, M. Engineering Thermofluids Thermodynamics, Fluid mechanics, and Heat Transfer. Berlin Heidelberg: Springer-Verlag; 2005.

[6] Moran, M.j., Shapiro, H.N. Fundamentals of Engineering Thermodynamics. Fifth Edition. Hoboken, New Jersey: John Wiley & Sons; 2004.

[7] Ekroth, I., Granryd, E. Tillämpad termodynamik. Edition 1:3. Lund: Studentlitteratur; 2006.

[8] Incropera, F.P., Dewitt D.P., Bergman, T.L., Lavine, A.S. Principles of HEAT and MASS TRANSFER. Seventh Edition. Hoboken, New Jersey: John Wiley & Sons; 2013.

[9] Bejan, A., Kraus, A.D. HEAT TRANSFER HANDBOOK. Hoboken, New Jersey: John Wiley & Sons; 2003

[10] Patil, R.K., Shende, B.W., Ghosh, P.K. Designing a helical-coil heat exchanger. Chemical engineering. 1982;89(25):85-88.

[11] Thome, J.R. Engineering Data Book III [ONLINE]. Decatur; Wolverine tube inc; 2004. [cited 2017 may 15] Available from `http://web.iitd.ac.in/~pmvs/courses/mel725/flowboil.pdf`

[12] Lemort, V., Guillaume, L., Legros, A., Declaye, S., Quoilin, S. A comparison of piston, screw and scroll expanders for small scale Rankine cycle systems. Pro-

ceedings of the 3rd International Conference on Microgeneration and Related Technologies. April 15-17, 2013; Napoli, Italy.

[13] Atkins,T., Escudie, M. A Dictionary of Mechanical Engineering [ONLINE]. Oxford: Oxford University Press; 2013. [cited 2017 April 26]. Available from http://www.oxfordreference.com/view/10.1093/acref/9780199587438.001.0001/acref-9780199587438-e-1053?rskey=z0qIkQ&result=1

[14] Kandlikar, S.G. A General Correlation for Saturated Two-Phase Flow Boiling Heat Transfer Inside Horizontal and Vertical Tubes. Journal of Heat Transfer. 1990;112(1):219-228

[15] Nouman, J. Comparative studies and analyses of working fluids for Organic Rankine cycles - ORC [master's thesis on the internet]. Stockholm: KTH Royal Institute of Technology. 2012 [cited 2017 March 30]. Available from http://www.diva-portal.org/smash/get/diva2:555314/FULLTEXT01.pdf

[16] Seher, D., Lengenfelder, T., Gerhardt, J., Eisenmenger, N., Hackner, M., and Krinn, I. Waste Heat Recovery for Commercial Vehicles with a Rankine Process. 21st Aachen Colloquium on Automobile and Engine Technology. October 7-9, 2012; Aachen, Germany.

[17] CoolProp. Pure and Pseudo-Pure fluid properties [ONLINE]. Available at: http://www.coolprop.org/fluid_properties/PurePseudoPure.html#list-of-fluids. [cited 24 May 2017]

[18] Hilpert, R. Wärmeabgabe von geheizten Drähten und Rohren im Luftstrom. Forschung auf dem Gebiet des Ingenieurwesens A. 1933;4(5):215-224

[19] Klimenko, V.V. A generalized correlation for two-phase forced flow heat transfer - second assessment. International Journal of Heat and Mass Transfer. 1990;33(10):2073-2088.

[20] Hasans I.H, Hasan H.M., Ghassan A.A. Study of the axial heat conduction in parallel flow microchannel heat exchanger. Journal of King Saud University - Engineering Sciences. 2014;26(2):122-131

[21] Lin, T.Y, Kandlikar S.G. A Theoretical Model for Axial Heat Conduction Effects During Single-Phase Flow in Microchannels. Jornal of Heat Transfer. 2011;134(2).

[22] Xuan Y., Roetzel W. Stationary and dynamic simulation of multipass shell and tube heat exchangers with the dispersion model for both fluids. International Journal of Heat and Mass Transfer. 1993;36(17):4221-4231.

[23] Hanuzkiewicz-Drapala, M., Bury T., Widziewicz, K. Analysis of radiative heat transfer impact in cross-flow tube and fin heat exchangers. First edition. Hoboken, New Jersey. John Wiley & Sons; 2003

[24] Shampine, F.L., Reichelt M.W. THE MATLAB ODE SUITE. SIAM Journal of Scientific Computing. 18(1):1-22

[25] CoolProp. Tabular Interpolation [ONLINE]. Available at: http://www.coolprop.org/coolprop/Tabular.html. [cited 28 April 2017]